SANDIA REPORT

SAND2014-0877
Unlimited Release
Printed February 2014

Manufacturing Process Modeling for Composite Materials and Structures, Sandia Blade Reliability Collaborative Phase II: Effects of Defects, Interim Report

Daniel A. Guest and Douglas S. Cairns, PI
Montana State University
Mechanical and Industrial Engineering
Bozeman, MT 59715

Sandia Technical Monitor: Joshua A. Paquette

Prepared by
Sandia National Laboratories
Albuquerque, New Mexico 87185 and Livermore, California 94550

Sandia National Laboratories is a multi-program laboratory managed and operated by Sandia Corporation, a wholly owned subsidiary of Lockheed Martin Corporation, for the U.S. Department of Energy's National Nuclear Security Administration under contract DE-AC04-94AL85000.

Sandia National Laboratories

Issued by Sandia National Laboratories, operated for the United States Department of Energy by Sandia Corporation.

Printed in the United States of America. This report has been reproduced directly from the best available copy.

Available to DOE and DOE contractors from
U.S. Department of Energy
Office of Scientific and Technical Information
P.O. Box 62
Oak Ridge, TN 37831

Telephone: (865) 576-8401
Facsimile: (865) 576-5728
E-Mail: reports@adonis.osti.gov
Online ordering: http://www.osti.gov/bridge

Available to the public from
U.S. Department of Commerce
National Technical Information Service
5285 Port Royal Rd.
Springfield, VA 22161

Telephone: (800) 553-6847
Facsimile: (703) 605-6900
E-Mail: orders@ntis.fedworld.gov
Online order: http://www.ntis.gov/help/ordermethods.asp?loc=7-4-0#online

SAND2014-0877
Unlimited Release
Printed February 2012

Manufacturing Process Modeling for Composite Materials and Structures, Sandia Blade Reliability Collaborative Phase II: Effects of Defects, Interim Report

Daniel A. Guest and Douglas S. Cairns (Principal Investigator)
Montana State University
Mechanical and Industrial Engineering
Bozeman, MT 59715

Sandia Technical Monitor: Joshua A. Paquette

Abstract

The increased use and interest in wind energy over the last few years has necessitated an increase in the manufacturing of wind turbine blades. This increase in manufacturing has in many ways out stepped the current understanding of not only the materials used but also the manufacturing methods used to construct composite laminates. The goal of this study is to develop a list of process parameters which influence the quality of composite laminates manufactured using vacuum assisted resin transfer molding and to evaluate how they influence laminate quality. Known to be primary factors for the manufacturing process are resin flow rate and vacuum pressure. An incorrect balance of these parameters will often cause porosity or voids in laminates that ultimately degrade the strength of the composite. Fiber waviness has also been seen as a major contributor to failures in wind turbine blades and is often the effect of mishandling during the lay-up process. Based on laboratory tests conducted, a relationship between these parameters and laminate quality has been established which will be a valuable tool in developing best practices and standard procedures for the manufacture of wind turbine blade composites.

Acknowledgements

This work was sponsored by Sandia National Laboratories (SNL) – Wind Energy Technology through funding from the United States Department of Energy (DOE) Wind and Water Power Technologies Program Office. The authors would like to thank Mr. Joshua A. Paquette and Dr. Daniel Laird of Sandia National Laboratories for guiding this work. In particular, we would like to thank Mr. Paquette from SNL for providing insight for the Sandia-led wind turbine Blade Reliability Collaborative (BRC). Also, Mr. Cash Fitzpatrick from DOE was particularly helpful in providing resources for the equipment used for quantitative process monitoring. Without this equipment, it would not have been possible to develop the experimental/analytical correlations of the process models developed herein. The authors acknowledge the observations and data provided by Mr. Steve Nolet of TPI Composites for his insight of porosity during composite structures manufacturing.

Table of Contents

Figures

Tables

1. INTRODUCTION

Over the past several years, the industry of manufacturing composite materials has undergone considerable improvement as the demands on the end product of composite laminates have increased. In some situations this increasing demand has seen the restructuring of manufacturing facilities that previously produced products such as boat hulls, and which now predominantly produce wind turbine blades and wind turbine blade molds. The advent of composite wind turbine blades and aerospace applications of composite materials has necessitated research into not only improving material properties through material development, but also developing new manufacturing techniques. Extensive research work has been done to model different aspects of the manufacturing process including laminate infusion techniques, fabric permeability variations, fluid flow modeling, and cure temperature profile optimization, [1-8]. Most of these previous studies have been approached from an analytical prospective and have been very focused on discreet aspects of the process. The end result is that for a specific situation, materials, infusion process, etc. results can be obtained which validate a given model but on a more global scale may not necessarily provide reliable results. Wind turbine blade manufacturers continue to encounter catastrophic blade failures that often affect the entire system was well as present a potential hazard, [9, 10]. As the demand for alternative energy increases and wind turbine blades are designed with increasingly longer lengths, the design window for structural demands to balance with increasing weight begins to shrink. As seen in Figure 1 some of the larger off-shore wind turbine blades can have blades as long as the span of an Airbus 380. New methods for refining the manufacturing process are needed in order to produce higher quality wind turbine blades.

Figure 1: Example of an 80-meter, offshore wind turbine.

The motivation for this research stems from the BRC (Blade Reliability Collaborative) Effects of Defects study conducted by several graduate and doctoral students at Montana State University. Some of the goals of that study have been to characterize the flaws found in wind turbine blades due to manufacturing defects, develop Finite Element Analysis (FEA) models to study the constituent behavior of the materials, and design tools that can be used to assess flaws in the field or post manufacturing, [11-14]. Research for the BRC Effects of Defect study involved manufacturing flawed samples, both wave flaws and porosity flaws, and then testing them to ultimate failure to provide reduced material properties and knockdown factors that can be used by blade manufacturers to assess flawed blades. Other research has focused on embedding sensors for cure monitoring, and in-service monitoring of wind turbine blades, [15]. A new approach is needed to analyze each of the steps in the manufacturing process in an effort to pinpoint the primary factors that govern the introduction of flaws. Current instrumentation used in the manufacturing process is somewhat inadequate in terms of measuring or detecting processes that might lead to the introduction of flaws. If quantifiable measurements could be made during the manufacturing process, a Statistical Process Control (SPC) analysis could be utilized to improve quality control techniques. This type of instrumentation could be used to not only monitor system process parameters but also to control the outcome of the process and decrease or eliminate scrap rates. Therefore, this research will focus on the manufacturing science associated with wind turbine blade composites and the processes that lead to these flaws found in wind turbine blades.

Modern wind turbine blades are manufactured using composite materials, which have a much higher strength to weight ratio. As the term "composites" suggests, this material is composed of two parts, structural glass or carbon fibers and a binding matrix system to hold the fibers in place. The processes required to manufacture these materials demands a precision that the industry has not been willing to afford and so shortcuts in the manufacturing process have led to the introduction of flaws. These flaws are manifested in one of two ways, fiber waviness, which is a localized misalignment of fibers, or porosity, which appears in laminates as opaque or white areas. Most of the failures that occur in wind turbine blades are initiated by one of these two flaws. Due to the catastrophic nature in which glass fiber reinforced composites fail, failures can propagate very quickly through the structure. Minimizing or eliminating the occurrence of these flaws due to manufacturing processes has been an ongoing goal for not only the research community but also the blade industry. A new approach is needed to analyze each of the steps in this process in an effort to pinpoint the primary factors that govern the introduction of flaws.

The initial steps in this evaluation were focused on identifying the manufacturing parameters which affect the quality of the laminate and in developing procedures and instrumentation for controlling and monitoring these parameters. Tests were conducted to capture critical information about the influence of each of the parameters and subsequently correlated to laminate strength. Work was also done to develop the questioning protocols for the implementation of an expert system diagnostic tool that could be used by technicians to troubleshoot flawed laminates.

An expert system, a form of artificial intelligence, is essentially composed of a knowledge base that is built from the experience of a human expert, if-then statements, and an inference engine that makes the connection between the knowledge and the rules. Through a series of questions the system is able to make judgments on which action should be taken or a determination of outcome. Examples of the application for expert systems range from medical diagnosis tools and protein identification systems, to crop management systems, and closed loop controllers, [16-19].

In this application the goal was to develop a system that will be able to inform technicians about the cause of manufactured flaws and ultimately educate them on proper manufacturing techniques. Tests were performed to rate the effects various process parameters have on laminate quality and to develop the knowledge or rules needed to build the expert system.

2. BACKGROUND

2.1. Manufacturing Materials & Methodology

For the last several decades the wind turbine blade industry has been challenged to produce increasingly larger blades with the capability of generating more and more power. Governments have begun to back the push for “green energy” with capital incentives for industries that employ this type of energy, [20]. This has led to the demand that is now driving these wind turbine manufacturers to extract a higher energy density from the installation of a turbine. Based on the mechanical limitations of the turbine generators themselves, blade manufacturers have been given the task of designing longer blades capable of capturing more wind energy. These larger blades do not however come without design challenges.

With the increase of the length of wind turbine blades comes a higher demand on the materials used to make them, [21, 22]. The typical loads that are seen in wind turbine blade operation are still inherent in today’s blades, such as bending and twisting due to the wind loads as well as radial or span-wise stresses due to high rotational velocities at the tips. Now with ever increasing length, the tip velocities are increasing which adds more stress, and with the increased length there is a substantial increase in weight. The larger the blade obviously there will be a greater inertial mass.

With this increase in mass and other associated stresses the blade structure itself is required to carry more loads. Therefore the design of the skins and shear web structures has to improve to meet these demands. For the last few decades blade design has seen an increased use of fiber composite materials due to their superior strength to weight ratio. These composite materials have allowed designers to push the limits of traditional wood or metal blades to larger blade designs. The key to the increased strength is that fiber composite laminates employ a very strong lightweight fiber, primarily either glass or carbon, and some kind of binding matrix material. The matrix material is able to transfer bending as well as axial loads to the fiber by constraining the fibers to a rigid shape. In figure 2 we see a micrograph of a typical composite laminate used in the construction of wind turbine blades. The lighter spots are the fiber ends while the dark regions are the supporting matrix material.

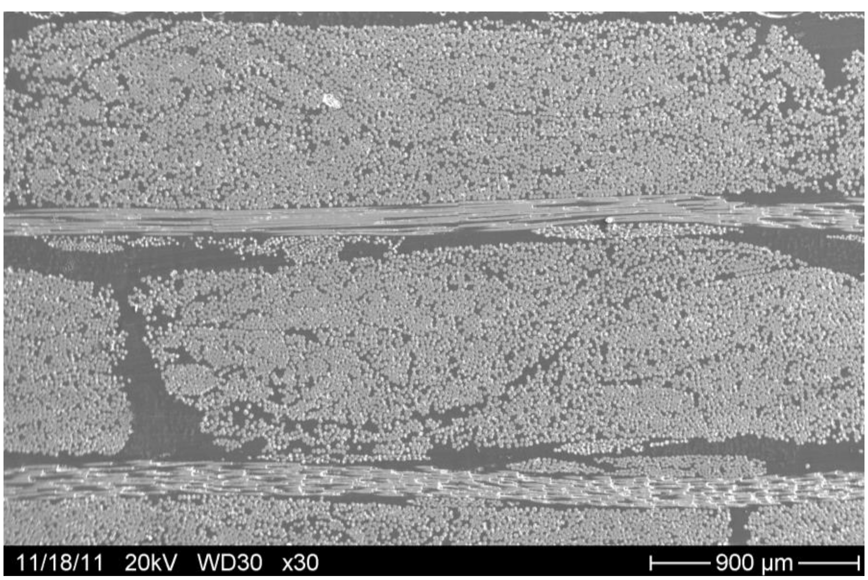

Figure 2: Micrograph of glass fiber composite laminate used in wind turbine blades.

2.2. Fabrics

The purpose of the fiber in a composite laminate is to carry the majority of the loads applied to the part. Since loading scenarios for a given part can vary widely with application, fabric types and architecture also vary widely. A unidirectional fabric for example is ideally suited in situations where the loads are only occurring in one direction whereas a biax fabric might be more applicable for parts that experience torsion or multi-axial forces. There are often times when the primary concern is not strength but weight and thus a composite laminate could be constructed from continuous strand mat. Figure 3 shows some of the different types of fabric architectures available for laminate construction.

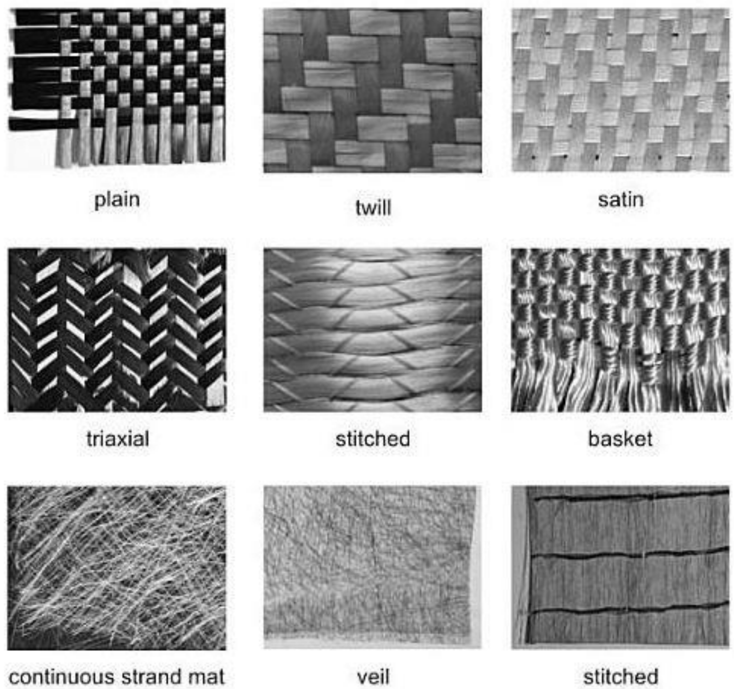

Figure 3: Fabric architecture [23].

The architecture of laminates manufactured from these different types of fabric becomes quite complicated requiring the use of a consistent orientation with the dominant loading directions. A system of global, (x-y-z) and local (1-2-3) coordinates has been adopted to make a distinction between the different layers and fiber directions, Figure 4. This becomes important to differentiate when considering the loads being transferred through the laminate as a whole as compared to the loading in one layer of the laminate. Loads will be carried differently in the global x-direction by the unidirectional fabric than they will by the ±45 (biax) fabric.

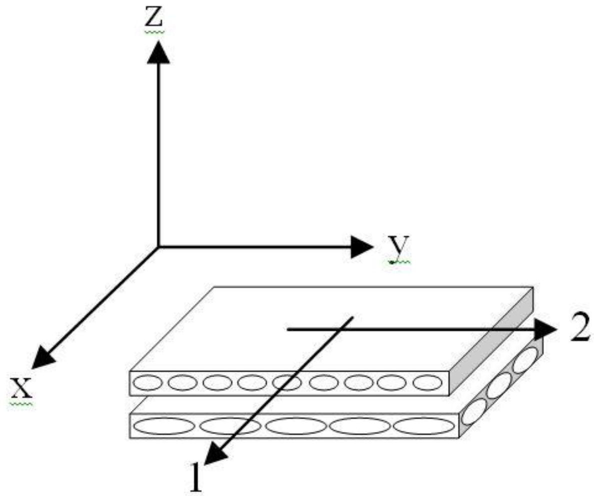

Figure 4: Global "laminate" coordinates versus local "lamina" coordinates.

An understanding of a standard coordinate system also becomes necessary when considering stacking of fabric layers and flaw orientations.

2.3. Matrix System

The matrix system used in a composite is very important and can be tailored to the cost and strength performance requirements of the specific part. The choice of matrix material can determine a laminates thermal, conductivity, cost, manufacturing, and mechanical characteristics. The purpose of the matrix material is to constrain the reinforcing fibers so that the load can be transferred to the fibers. In the case of shear and compression loads the matrix dominates in terms of load carrying, which makes the type of matrix material, used very important. In Figure 5 a micro graph of the cross section of a glass fiber laminate shows the interaction between the fiber and the matrix.

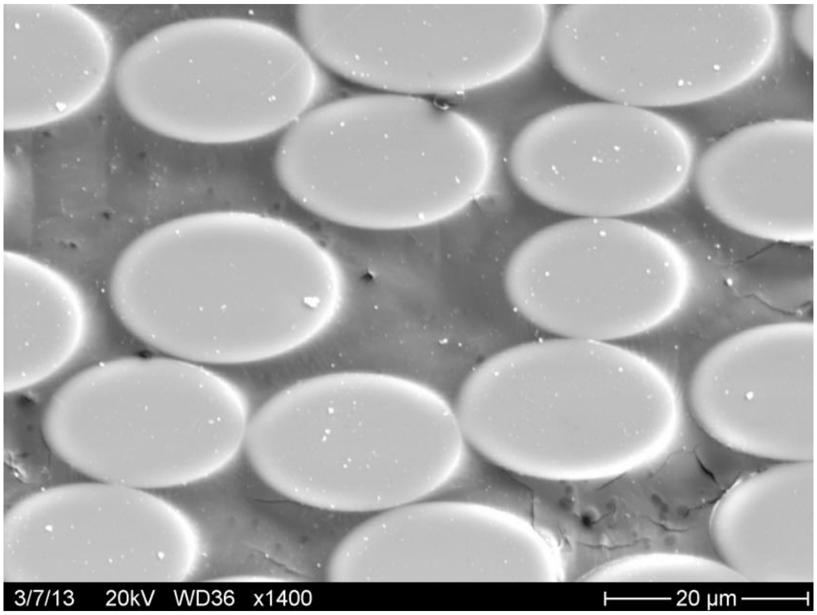

Figure 5: Micrograph of glass fibers in a matrix material.

Depending on the application a thermoset or thermoplastic matrix can be used, the most common being thermosets because of the ease of processing. Epoxy resins are a thermoset most commonly used in wind turbine blades due to their high mechanical properties, low viscosity, and high corrosion resistance[23].

2.4. Blade Manufacturing Process

There are two methods of manufacturing composite laminates, which are widely used in the wind industry. The first method involves using prepreg material with vacuum compaction, and the other employs the use of dry fibers again with vacuum compaction, which also assists in the transfer of resin through the dry fiber. This second method known as Vacuum Assisted Resin Transfer Molding (VARTM) is typically used by blade manufacturers for manufacturing wind turbine blade composites[24]. The basic procedure for constructing laminates in this way is to infuse dry fibers, either glass or carbon, with the binding matrix, which is usually an epoxy, resin system. This hard/soft mold process requires that the dry fibers be initially "laid up" in a hard mold that will be the final shape of the part. In Figure 6 workers at TPI, a composite wind turbine blade mold manufacturing company in Rhode Island, are laying-up the dry fibers for one of the MSU composite group's BRC effects of defects blades. These blades were later tested at NREL (National Renewable Energy Laboratory) in Boulder, CO in fatigue testing.

Figure 6: Workers at TPI laying up dry, fiberglass fabric for a BRC test blade.

Along with the fabric blades, skins are constructed with some kind of core material placed in between layers of fabric on either side of the center spar cap fabric layers. As was the case of the BRC blades that were manufactured for MSU, balsa wood is typically used due to its ideal mechanical properties, not the least of which is its low weight.

Another important step in the process of constructing wind turbine blades is designing resin flow channels into the mold to allow resin to quickly saturate the fabric. This is accomplished using polymer tubing to direct the resin where it needs to start saturating the fabric. From there the flow media is placed to distribute the resin over the surface of the laminate. Finally, vacuum ports are strategically placed around the mold to direct the flow of resin so that all of the laminate will be saturated. Figure 7 shows these components of the lay-up process.

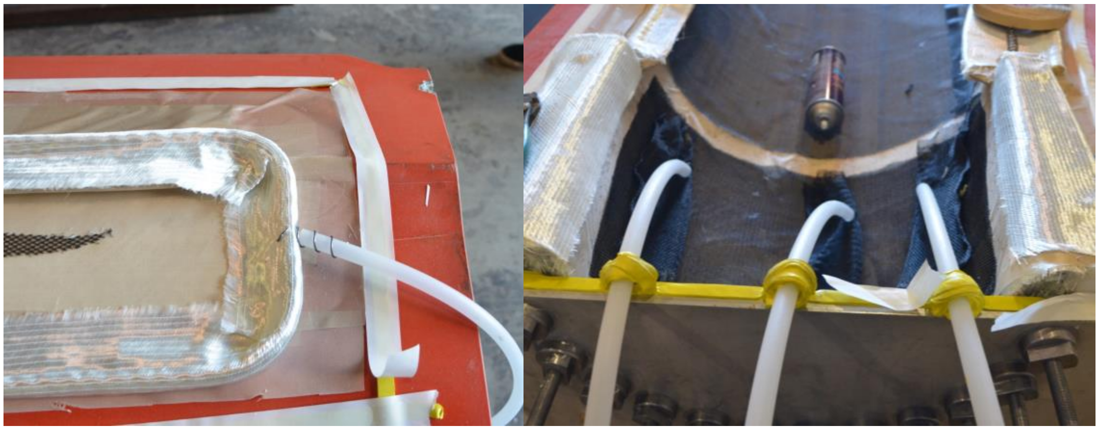

Figure 7: Vacuum ports are affixed to porous rope to direct and control the vacuum pressure (left). Injection ports (right) allow resin to enter the mold

Once all of the dry fiber is in place a polymer film is sealed over the mold using tacky tape around the entire perimeter of the mold, Figure 8. Wind turbine blade skins manufactured in this way are very costly due to the extensive labor involved, which necessitates a very thorough evaluation of every aspect of the process. Once the vacuum bag is taped down and vacuum is pulled, thorough tests are conducted to make sure that the vacuum holds for the time it will take to cure the part in the mold.

Figure 8: Technicians at TPI applying vacuum bag to the mold of one half of a BRC blade.

Using a pressure gauge, technicians at TPI are able to monitor any drop in vacuum pressure, which would indicate a leak. If a leak is suspected, an ultrasonic leak detection device is used to pin-point the location of the leak by probing the entire perimeter of the mold/bag interface, Figure 9.

Figure 9: Leak detection techniques include monitoring the quality of the vacuum over a period of time using a pressure gage (left); as well as an ultrasonic leak detection device (right).

Once assured of a good vacuum seal, the liquid resin is prepared by mixing the hardener with the epoxy resin and injected into the mold. Often technicians heat the resin before injecting it into the mold to decrease the viscosity of the resin; this allows it to permeate the dry fibers more easily. In Figure 10, the completed mold is ready for resin infusion.

Figure 10: Completed laminate under vacuum seal and ready for resin injection.

Modified vise-grip clamps are used to seal the ports or control the flow of resin through the various ports in the mold. After the blade has been fully saturated with resin, these clamps are used to seal off the tubes so that air cannot leak into the mold, Figure 11. At TPI the resin for each of the half blade shells was mixed in very large tubs and then transferred to 5 gallon buckets that were placed at each of the injection ports around the mold. Once the infusion process was started technicians would remove the clamps from the hoses while the end of the hose was immersed in the 5 gallon bucket of resin.

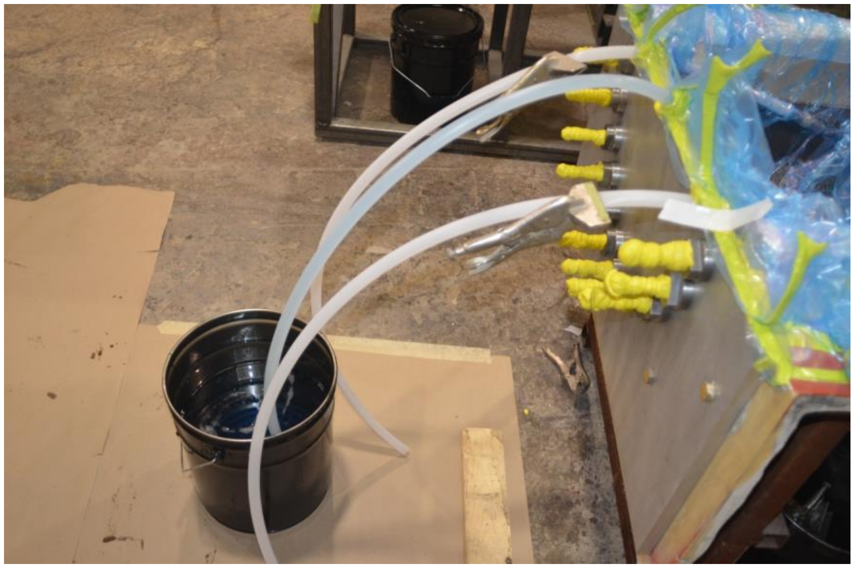

Figure 11: Resin is mixed in large pails, and then transferred to 5-gallon buckets during the injection process. Modified, vise-grip clamps are used to control the flow of resin and to seal the vacuum and injection tubes when not in use.

The completed parts of the blade are later trimmed, cleaned and readied for assembly. The parts are ultimately assembled using adhesives to bond the two shells and the shear web together. Completed blades are manufactured with a gel coat as the first layer in the mold, which gives the blades a glossy sheen. Figure 12 shows one of the completed blades manufacture at TPI during the summer of 2012.

Once the laminates have cured and the blades are assembled, there has been a significant amount of money invested into a blade, which is why special attention should be taken to fine tune all aspects of the manufacturing process. In addition to economic issues, other manufacturing issues are of concern as well.

Figure 12: Completed blade manufactured at TPI.

2.5. Manufacturing Issues

One of the biggest concerns that wind turbine blade manufacturers' face today is maximizing strength while minimizing weight associated with over design. Typically blades are structurally over designed, in part to account for inevitable flaws that are associated with the manufacturing process. These inevitable flaws can often lead to catastrophic failure of the blades, which can damage not only the blades themselves but also the tower that supports them. Figure 13 below, illustrates wind turbine blades manufactured by Vestas which suffered failure due to manufacturing defects.

Figure 13: Wind turbine blades manufactured by Vestas which suffered failure due to manufacturing defects, [25].

2.5.1. Typical Laminate Flaws

Within the manufacturing process of composite laminates, there are two main contributors to the flaws that ultimately result in wind turbine blade failures: fiber misalignment and porosity (or voids). These two types of flaws are the root cause of all premature wind-turbine blade failures found in the industry and, if eliminated or at least minimized, could greatly impact the profitability and reliability of composite wind turbine blades, [11-14]. Due to the anisotropic nature of composite materials, fiber misalignment can be thought of as two separate categories of flaws: Out-of-plane waves (OP waves), which are misalignments in the z-dir or out of the plane of the laminate, and In-plane waves (IP waves), which are misalignments in the y-dir or in the plane of the laminate.

Flaws of the OP wave category are typically introduced when producing thicker laminates such as those used for the root section of a wind turbine blade. The flaws are introduced when a small perturbation in the fabric is amplified through the layers. If the flaw goes unnoticed, it can grow into significant waves and even wrinkles. Examples of the waviness that has been found in full scale wind turbine blades can be seen in Figure 14. These types of flaws are most often the result of mishandling of the fabric while it is being laid up in the mold. Often during the lay-up process, layers of fabric are sprayed with an adhesive, Super 77, which helps to hold the layers in place. Hypothetically, during this process is most likely when the first wave occurs and from there propogates through the other layers.

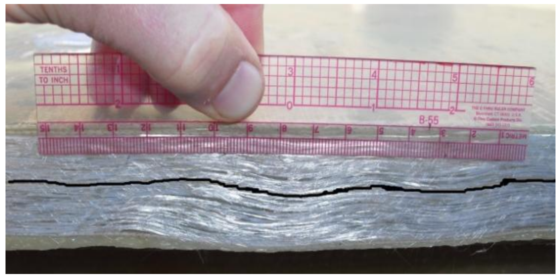

Figure 14: OP wave flaws found in the skin of wind turbine blades[13].

On the other hand, in plane waves can occur anywhere in a laminate and are caused by a variety of things. Obvious causes of IP waves are from mishandling the fibers while they are being placed in the mold, fibers first starting as OP waves and getting flattened out into IP waves, or from dragging a foreign object across the fabric. A less common cause of IP waves is fiber washout, which is typically waviness caused by using the Resin Transfer Molding RTM process. Fiber washout however, is less likely to occur using the VARTM process since the fabric is being held tightly by the vacuum bag. An example of an IP wave can be seen in Figure 15. The flaw pictured was most likely due to mishandling the fabric while it was being inserted into the mold.

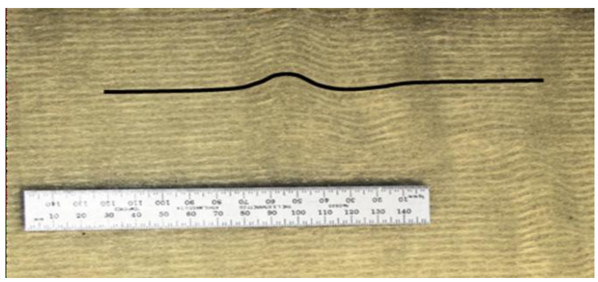

Figure 15: IP wave flaw found on the surface layer of a wind turbine blade skin[13].

The third and most complicated flaw type is porosity. Its complexity arises from the fact that there are a number of different probable causes for the introduction of porosity in a laminate. The two main contributions are leaks and infusion control. While it is obvious how leaks can cause problems and further how they are relatively simple to mitigate, controlling the infusion process involves a number of different manufacturing parameters. The vacuum infusion process can result in what are known as dry spots or voids, which can be caused by a couple of different mechanisms. The main problem is that if the flow is not controlled correctly, encapsulation can occur which traps dry pockets in the fabric. At this point it is necessary to develop what are known as process parameters which are the primary contributors to laminate porosity.

2.5.2. Process Parameters

The idea of process parameters has been investigated for composite laminates and is determined to consist of time, temperature, and pressure [7]. Process parameters are the factors that have been determined by observation to influence the introduction of void inclusions in laminates. Based on observations of the manufacturing processes employed by MSU's composites group as well as the composite manufacturers at TPI, process parameters considered for this study would encompass the following aspects specific to the VARTM process used to manufacture wind turbine blades: resin temperature, laminate architecture, layers of fabric, layers of flow media, vacuum pressure, resin flow rate, and degas status. These are the parameters which the current research has deemed to most likely effect the quality of the laminate as it pertains to the manufacturing process.

Resin temperature was chosen as one of the parameters due to its direct correlation to resin viscosity. If the viscosity of the resin could be sufficiently decreased, then the effective permeability of the fabric would increase; subsequently, there would be less chance for encapsulation to occur. Research on the manufacturer's website documents the supposition that the resin viscosity could be controlled by changing the temperature of the resin, Figure 16.

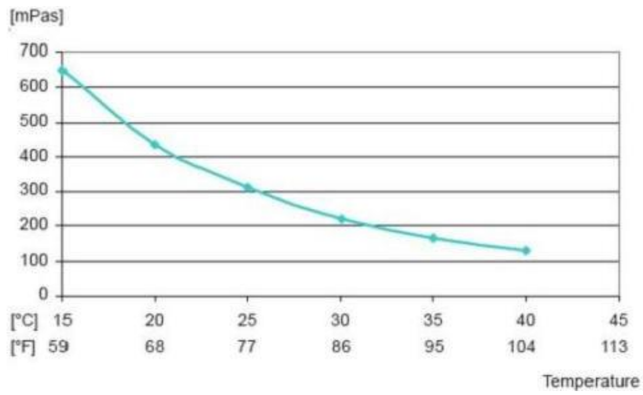

Figure 16: Momentive data for the RIMR 135 resin system used in this study [26]. Plot shows viscosity as a function of temperature.

2.5.3. Outcome of Process

Regardless of the type of flaw present in a composite laminate, the governing metric for categorizing composites is the laminate quality. This terminology will be used throughout the rest of this report to refer to the outcome of the manufacturing process. A high quality laminate is distinguished as one that is devoid of defects whether it is a wave flaw or porosity flaw. When porosity flaws are considered, laminate quality will directly relate the percent of porosity contained in the laminate, whereas for wave flaws, the wave angle will determine the degree of flaw. The porosity content values can be reported in one of two ways: % porosity by matrix or % porosity by volume (or by the volume of the entire laminate which includes the fiber volume). To maintain consistency with other research, percent porosity by volume will be reported here where applicable.

2.6. Modeling

The term modeling as it is used in the application for fiber composite manufacturing refers to a tool that can be used to mimic or simulate the actual process of manufacturing a composite laminate. A mathematical model then provides a means of predicting an outcome based on mathematical algorithms. In consideration of the manufacturing process associated with composite wind turbine blades, a brief discussion of previous modeling efforts will be presented.

2.6.1. Numerical Modeling of Resin Flow

Commonly, numerical models employ flow modeling equations such as Darcy's Law, [1, 3, 7, 27-31]. For the RTM process, Darcy's Law relates the volumetric flow velocity to the pressure gradient inside the mold with proportionality constants such as resin viscosity and fabric permeability. These models provide a means of predicting optimum flow velocities with respect to pressure gradients in the mold. Some of studies have modeled the use of multiple injection and vacuum ports to control void formation due to convergent flow fronts, [32]. The modeling methods and equations used are quite common and can be particularly useful given specific conditions. The goal of this research was to provide a new approach to the modeling process that could be easily applied to a variety of manufacturing processes.

3. EXPERIMENTAL SETUP AND EQUIPMENT

3.1. Materials

3.1.1. Fabrics

Effort was made in the manufacturing of the experimental plates to maintain consistency with the material types used in the wind turbine blade industry. Since the impetus for this research has been to understand the influence of manufacturing processes on the wind turbine blade industry, fabrics that are commonly used by the industry were chosen. The primary fabric used in the study of defects in wind turbine blades has been a unidirectional fabric produced by Devold called PPG-Devold L1200/G30-E07. This fabric was used for its high fiber weight and Figure 17 shows the front, predominantly zero lamina direction, of the fabric in the left image. The back side of this fabric, as seen in the right image, has a small amount of 90º fibers and random matting, which combined with the stitching help to hold the toe bundles together.

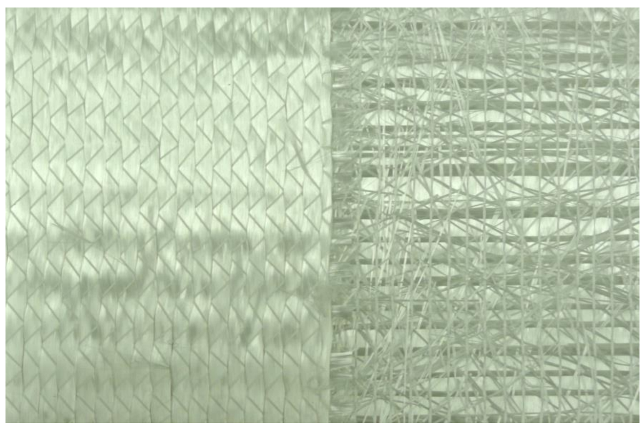

Figure 17: PPG-Devold L1200/G30-E07 fabric.

The second fabric that was be used in this study is a biax fabric produced by Vectorply called Vectorply E-BX 0900-10. This fabric combined with the unidirectional PPG fabric was used to simulate a triax fabric that is commonly used in wind turbine blades. These fabrics were chosen due to the similar material properties and fabric weights to the triax material. In Figure 18, the architecture of the biax fabric can be seen.

Figure 18: Depiction of the Vectorply E-BX 0900-10 fabirc.

Other fabrics necessary for the construction of composite laminates using the vacuum assisted resin transfer molding, (VARTM) process include flow media and peel ply. There are many different types of these fabrics used in industry; however, they all serve one primary purpose which is to disperse the resin through the laminate as efficiently as possible. Due to the large variance in styles and brands, fabrics were chosen that were readily available in the laboratory at MSU. A material called Airtech Release Ply Super F (Polyester) is the common peel ply used. In the left image of Figure 19, this fabric can be seen being used on the top and bottom of the laminates. Peel ply is used for two different reasons. One is to achieve a better mechanical bond than would otherwise be impossible to get without it. The second purpose is to make de-tooling the laminate from the mold easier.

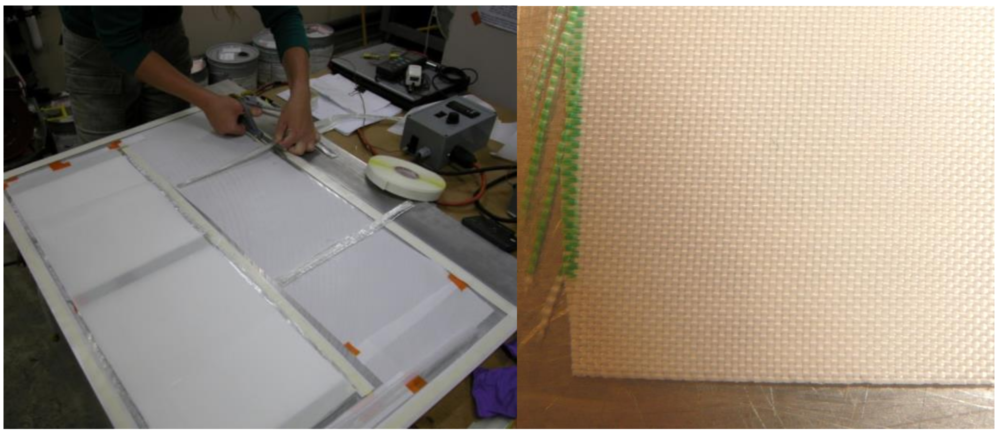

Figure 19: Peel ply is used for ease of de-tooling laminates as well as creating a better mechanical bond.

In the right image of Figure 19, the basket weave pattern that contributes to the texture that the laminates have after curing with this peel ply are illustrated. Because this fabric is made from polyester, the resins do not chemically bond to the fabric, which is why it is used as a "releasing layer."

The most common type of flow media found at the MSU's composites lab is Airtech Greenflow 75, a polypropylene material with an open mesh that allows the resin to easily flow through it during the infusion process. In the left image of Figure 20 the flow media is being added in the "lay-up" process while the right image shows the resin flowing through the flow media during the infusion process. Typically the flow media is held short of the end of the composite fabric to improve saturation at the end of the laminate.

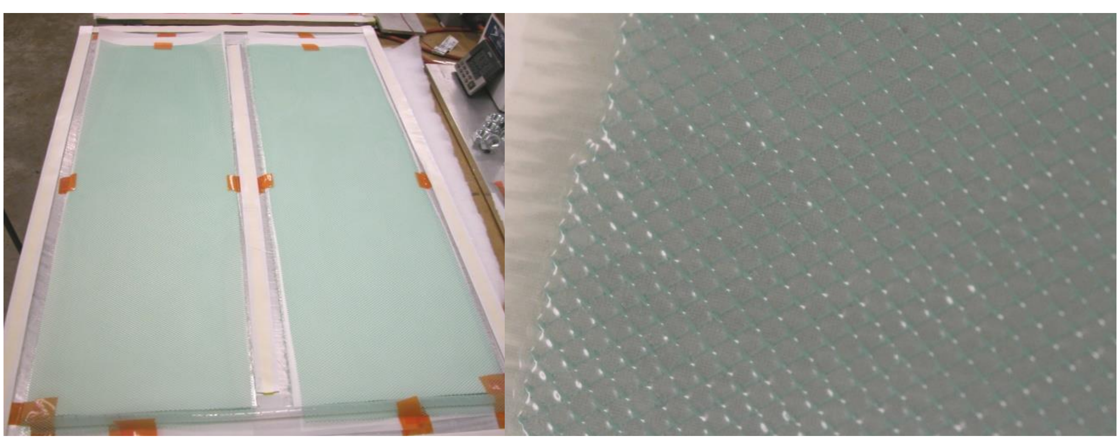

Figure 20: Left is flow media being used in the construction of a glass laminate. Right is a close up view of resin flowing through the open mesh of the flow media.

3.1.2. Resins

As with the fabrics, a resin system was used that most fully simulates those used in industry. The type of resin system selected was extremely important for a number of reasons: mechanical properties, pot life, and viscosity. First of all, because the mechanical properties of a resin system dictate its strength, a strong system was selected. Secondly, pot life was considered. RIMR 135 has a particularly long pot life and can remain workable for up to four hours; consequently, it is ideal for injecting large laminates like wind turbine blade shells which can take up to two hours to completely infuse from the time the resin is mixed. Last but not least, resin viscosity, one of the main manufacturing parameters targeted in this study, affected the resin system selected. To this end a Hexion Epoxy system called Hexion Epikote MGS® RIMR 135 along with the hardener RIMH 1366 were chosen for this study. The manufacturer's data sheet, depicted above in Figure 16, shows the correlation of resin viscosity to temperature.

3.2. Equipment

3.2.1. Hardware

Experimentation was conducted with a variety of different devices used for measuring and controlling temperature, pressure, and flow rate data. In the following section, the specific equipment used for this study of the manufacturing process of wind turbine blade composite laminates will be presented.

3.2.1.1. Endocal Heater/Chiller.

One of the parameters of the manufacturing process was the temperature of the resin system being injected into the laminate. As a means of controlling the temperature of the resin an Endocal RTE-5 refrigerated circulating bath, manufactured by Neslab, was used. These circulating baths have inlet and outlet ports on the side of the machine for circulating the fluid through an external vessel. In Figure 21 the bath is pictured in the left image while the ports are shown in the right image.

Figure 21: Endocal Refrigerated circulating bath.

Since it was necessary to both heat and cool the resin without contaminating the resin with the circulating fluid, the 3/8" external ports were utilized by connecting tubing between the ports and a 2 gallon bucket with 3/8" barbed fittings fixed in the side of the bucket. Figure 22 shows the bucket with the barbed ports and tubing attached. Inside the bucket spacers were added to keep the resin pail off the bottom of the bucket, so circulating fluid would pass on all the sides and the bottom of the resin pail. An added benefit was that it made putting the pale into the bucket easier.

Figure 22: Heat exchanger bucket for heating or cooling the resin.

Tacky tape was also used to seal around the fittings to make sure the circulating fluid did not leak out. The bucket had to be elevated so that the level of the fluid in the bucket was above the inlet and outlet ports on the side of the machine. If the bucket was not elevated, the fluid would all pump out of the Endocal heater/chiller and into the bucket, indicating that the inlet side of the machine was gravity fed. With the bucket elevated, Figure 23, the machine worked very well and achieved input temperatures very quickly.

Figure 23: Endocal heater/chiller with heat transfer bucket and tubing attached.

3.2.1.2. Vacuum Pump & Accessories.

The manufacturing method, used to produce wind turbine blades called Vacuum Resin Transfer Molding (VARTM), was used for this research in an effort to produce laminates consistent with industry standards. In order to manufacture laminates using VARTM, a vacuum pump was necessary along with some other specialized equipment. A 25 Hp Alcatel industrial use vacuum pump was used along with a resin trap to create the necessary vacuum pressure gradient needed to infuse laminates using this process. Figure 24 shows the vacuum pump on the left and the resin trap on the right. The primary purpose of the resin trap is to protect the pump from being damaged by resin that could be drawn up the line that far and get into the pump.

Figure 24: Alcatel Industrial vacuum pump and resin trap.

3.2.1.3. Scale

One of the main parameters believed to affect the outcome of composite laminates manufactured using the VARTM process is the flow rate of resin through the laminate. The only practical way to monitor this flow is to measure the resin flowing through the inlet tube using a flow meter of some kind. Several meters were researched in an attempt to find one that would not only be able to measure very slow flow rates but also not have to be in physical contact with the resin. Finally the best solution seemed to be to monitor the changing mass of resin in the mixing bucket. An Arlyn scale was used as seen in Figure 25. This scale had the capability of recording data using five different ways, data logging to an external USB flash drive, milliamp analog output, USB connection to the computer, RS-232 serial port to the computer, and Ethernet connection through a network.

Figure 25: Arlyn Scale used to monitor flow rate. Left is control panel, right is measurement platform.

After recording data from a couple of the experimental plates, it was determined that the data recorded using the analog output was not going to be accurate enough to report flow rate values since the error associated with this data was significantly larger than the range of flow rate values. After consulting with a manufacturer, it was determined that the analog outputs have an accuracy of 3000/1 while the other methods of logging data had an accuracy of 50000/1. Ultimately the USB flash drive data logging method was used for the sake of simplicity.

3.2.1.4. Pressure Transducers

Another one of the main parameters associated with the manufacturing process, closely tied to the flow rate, is the vacuum pressure and pressure gradient in the mold. As with the flow rate measurement, there was the restriction that this instrument had to either not contact the resin, or it had to be easily cleaned and not damaged by contact with the resin. After some research, miniature flush diaphragm pressure transducers were purchased from Omega, Figure 26. These transducers were absolute pressure sensors which allowed for pressure readings less than atmospheric pressure. Additionally, being flush mount devices, they were easily configured so as to minimize cleaning; and, therefore, minimize the amount of wear to the surface to the transducers.

Figure 26: Miniature flush diaphragm pressure transducer.

Figure 27 shows the transducer mounted in the mold next to the vacuum and injection port. Mounting the pressure sensors in this way made it easy to clean since the peel ply could be applied directly over the sensor. With a treatment of mold release, there was little resin left on the head of the transducer when the plates were de-tooled.

Figure 27: Mounting the transducers to the aluminum mold.

The pressure transducers required a 5 volt DC power source which was supplied by a Hewlett Packard 6234A dual output power supply. As seen in Figure 28, both transducers were powered from one of the outputs on the power supply. The rest of the connections for the transducer were made using the mating connector (Omega part number PT06F10-6S) and 15 feet of cable supplied by the manufacturer.

Figure 28: 6234A dual output Hewlett Packard power supply used to power the pressure transducers.

The manufacturer of the transducers supplied calibration measurements at 0, 50, and 100 psia along with the respective voltage outputs from which to calculate the sensitivity of each individual sensor. For this study, the data given was measured using an input voltage of 5.00 volts. Using this information each transducer was assigned an individual sensitivity value as seen in Table 1.

Table 1: Transducer sensitivity values see.

Transducer Model #:	202178	202181	
sensitivity (S-1):	0.0992	0.0859	mv/PSIA
sensitivity (S-2):	0.01984	0.01718	mv/V/PSIA

Having the sensitivity (S-2) value was important since the transducers were used on a different system and supply voltage than that which was used to initially calibrate them. A final voltage/pressure correlation was able to be made using the actual experimental voltages and these S-2 values.

3.2.1.5. IR Thermometer

One aspect of the manufacturing process that was believed would have a significant impact on laminate quality was the viscosity of the resin being infused into the laminate. Since viscosity is influenced by temperature, a method of controlling the temperature of the resin was sought. Therefore, for this study the resin temperature was monitored using an IR thermometer purchased from Omega, Figure 29. Using an IR thermometer allowed temperature measurements to be made without contaminating the sensor with resin. The temperature of the circulating bath was also monitored using this tool because it was important that there was no cross contamination.

Figure 29: An IR thermometer was used to monitor resin temperature. This reduced cleaning time for manufacturing plates.

3.2.1.6. DAQ System

Data from the various sources during manufacturing was collected using the National Instruments USB 6229 Data Acquisition system shown in Figure 30. The USB 6229 data acquisition system is a 16-bit multifunction input/output DAQ with 32 channels. This device is capable of handling input voltages of ±10 volts which was more than enough to acquire signals from the various equipment used for this experiment. Wiring the individual components to the DAQ required special attention to the type of signal being produced by that piece of equipment. Some of the connections needed to be grounded and some did not.

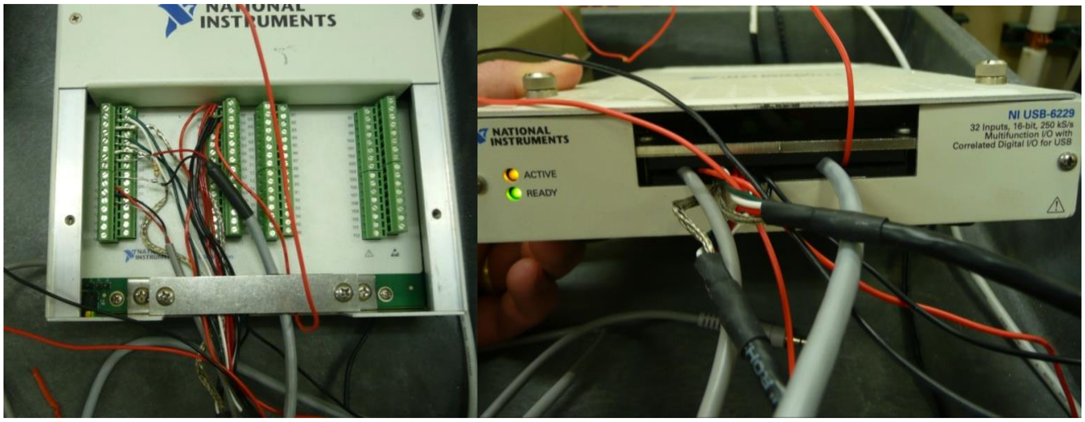

Figure 30: The National Instruments USB 6229 DAQ system was used to collect data from an IR thermometer, Arlyn Scale, and two pressure transducers.

To completely capture data from all of the sensors, five of the input channels were used. One channel was used to capture data from the scale (which ultimately was not used), one channel for both of the pressure transducers, one channel to monitor the power supply voltage, and one channel was used to record the resin temperature from the IR thermometer. The versatility of the DAQ devises made them ideal for this research and experimentation since they could be configured in a variety of ways depending on the application needed.

3.2.1.7. Mold

The mold used for this study was a flat 3/8”-thick plate with dimensions of 2’ x 3’. This was a milled-finish aluminum plate purchased from McMastercarr. To prepare the mold for use, the surface was sanded to an 800-grit finish; holes were drilled and tapped for the injection and vacuum ports, as well as, for the pressure transducers. Figure 31 clearly reveals that the holes for the ports were placed close to the transducers so that the pressure measurements at the two ends would be as true as possible.

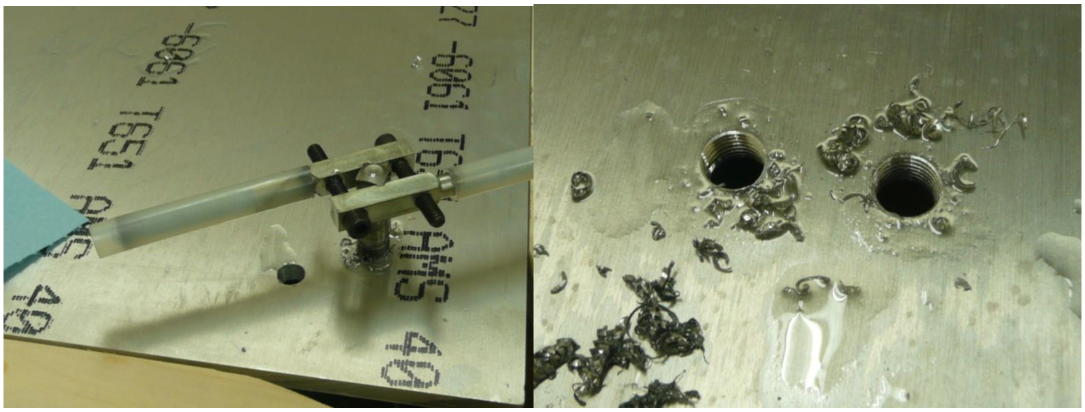

Figure 31: The mold was prepared for use by drilling and tapping holes for ports and transducers.

In order to reduce curing time, heater pads were purchased from Omega. Two 10” x 30” heater pads were adhered to the bottom of the mold and wire a cord to the heater leads. The purpose of the heater pads was to maintain a constant mold temperature of 77°F during the mold curing process because research has shown that curing at this temperature reduces curing time by 24 hours. In Figure 32, the heaters are shown with the cord wired to the leads. In the right image, the pads have been adhered to the bottom of the mold.

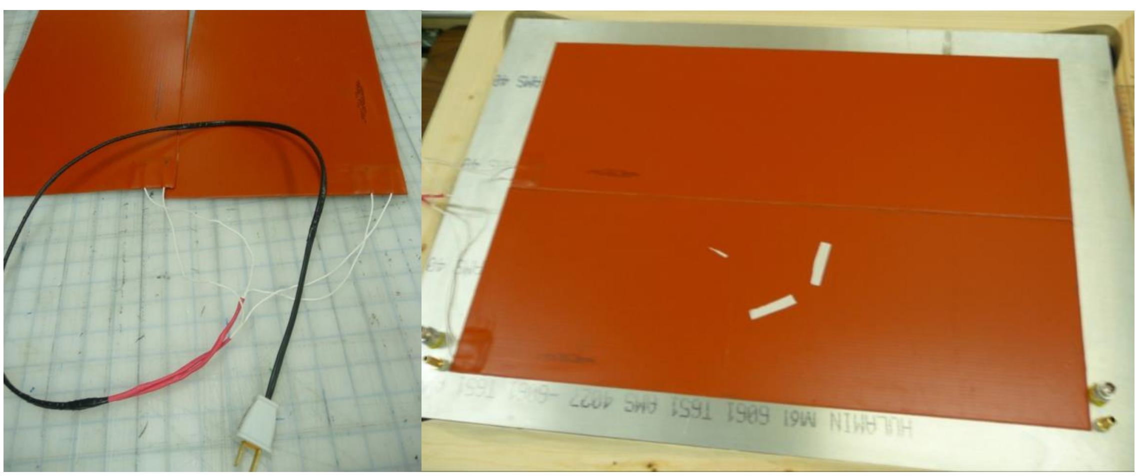

Figure 32: Flexible silicone rubber fiberglass insulated heaters used to control mold temperature while curing.

3.2.2. Software

Although data was to be acquired using the NI USB 6229 DAQ system to record information in a useful format, there was still a need to also visually monitor the information during the process. National Instruments Labview program was used to accomplish this task. Labview is a tool designed for scientists and engineers, which employs graphical programming and hardware integration to assist in experimentation. A virtual instrument (VI) was constructed to acquire the voltage signals and convert them into a meaningful format

3.2.2.1. National Instruments Labview

The VI that was created for this study was a simple while-loop structure as seen in the block diagram view of the program depicted in Figure 33.

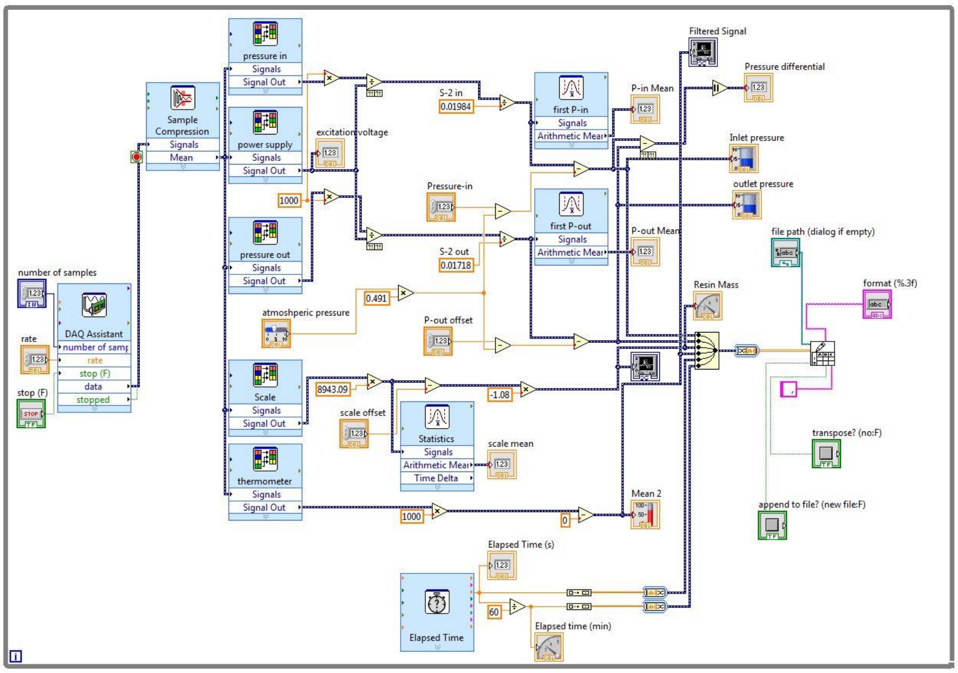

Figure 33: VI created for the acquisition, manipulation, and recoding of data taken during the manufacturing process study of wind turbine blade composite materials.

The first step in the data flow of that VI started with the DAQ Assistant, which was configured to acquire the individual signals from the channels that were specified during the components initialization or could later be selected under the properties menu, Figure 34.

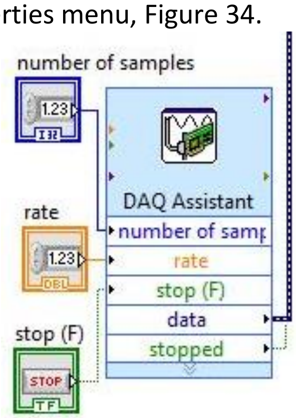

Figure 34: DAQ Assistant component of the program which collected data from individual channels of the hardware.

From the DAQ Assistant, the data was compressed to minimize some of the noise in the system and then it was split into the constituent signals which corresponded to the individual voltage signals coming from each device, Figure 35.

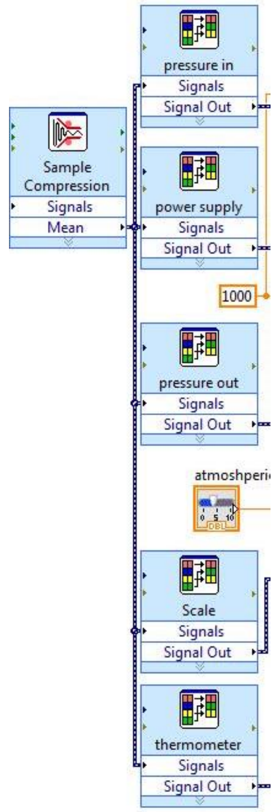

Figure 35: All the signals are compressed and then the channels are split apart for individual manipulation using Labview.

The individual voltage signals were then manipulated to indicate the appropriate output desired. For example, the signal from the pressure transducers, being a millivolt signal was multiplied by a thousand and then divided by the transducers input voltage which was the signal value from the power supply channel, Figure 36.

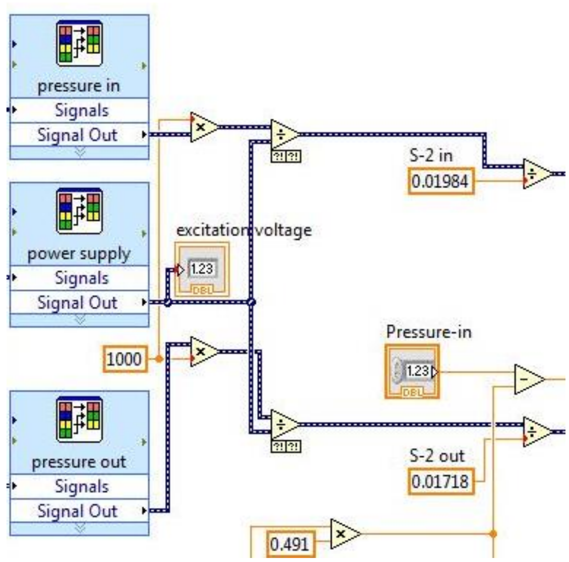

Figure 36: Pressure transducer signals were manipulated to produce a value of pressure from the voltage signal.

Voltage signals were divided by their constituent sensitivity values to covert to units of pressure in pounds per square inch (psi). The next step, in data flow, was to correct the output to current atmospheric pressure, calculate the pressure differential, and then to combine the two pressure signals, differential value, and the other three data strings using a merge tool, Figure 37. The output from the scale and the thermometer required similar signal manipulation to convert the voltage signals to temperature and mass values.

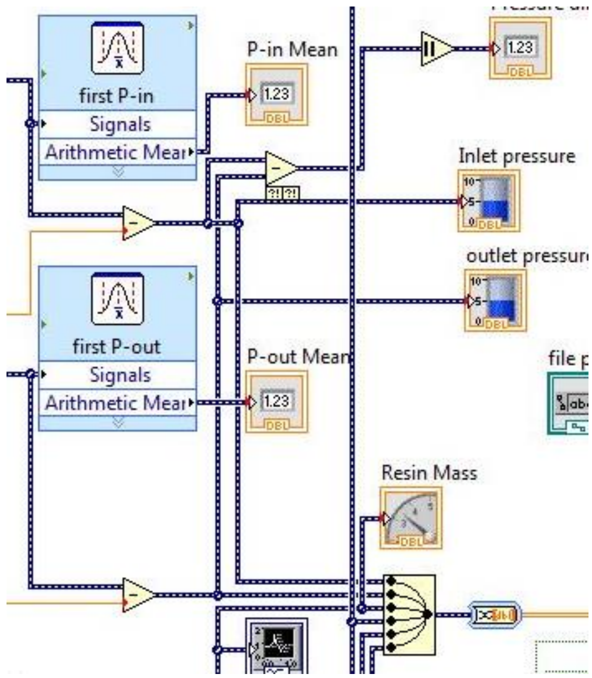

Figure 37: Elements used to calibrate the transducers to current atmospheric pressure conditions.

In the final step in the data flow of the VI, the VI wrote the data to an excel spreadsheet and continued the process until acquisition was terminated using the input controls on the front panel, Figure 38. The "write to spreadsheet" element gave the user options for controlling how the data was to be stored. For this experiment, the nodes for collecting 1-D data, specifying a file path, formatting the data, transposing the data into columns instead of rows, and appending data to the file were chosen. The "append to file" element was important when running the program in a loop structure since the default setting only captured the sample points from the last iteration of the loop. A delimiter element was also used to separate the output data into individual columns.

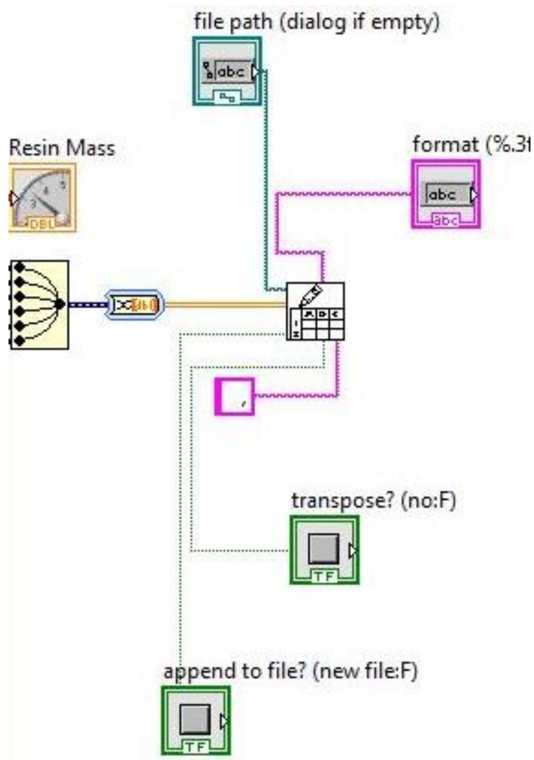

Figure 38: The "write-to-spreadsheet" element collected all of the data and saved it in the specified file.

Since the data written to the file did not carry any time stamp with it, components were added to create a time stamp, as well as, to monitor elapsed time. Displays were configured on the front panel to show elapse time in minutes and seconds, Figure 39.

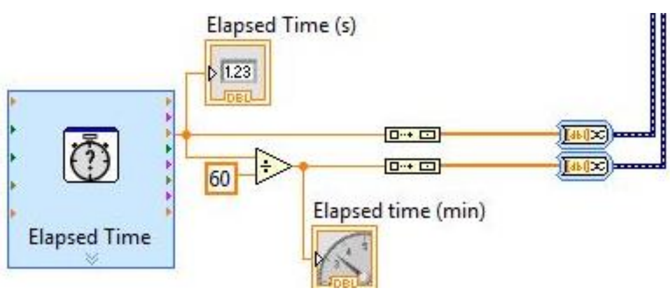

Figure 39: "Time stamp" elements were added to the data string.

The front panel of the VI was where the user controled the various parameters of the VI, such as setting the current atmospheric pressure, sampling rate or number of samples, as well as stopping and starting the collection of data. Figure 40 shows the front panel's graphical display of the pressure data, scale output, thermometer output, and elapsed time.

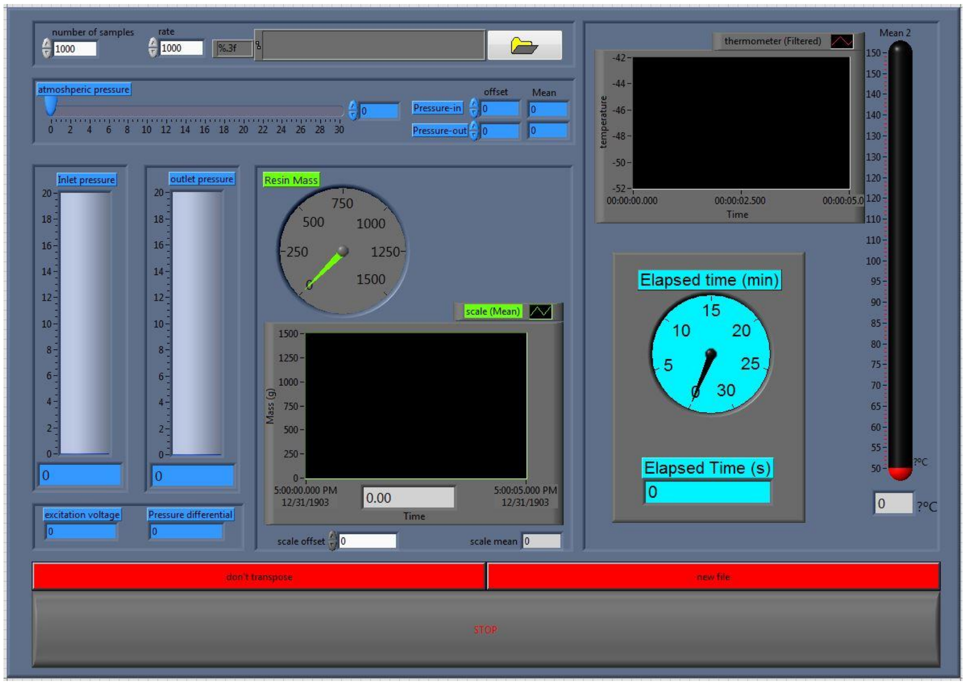

Figure 40: VI Front panel was used for controlling and monitoring the experimental data acquisition.

3.2.3. Equipment Summary

The equipment used for this research was chosen specific to the requirements of the various aspects of the manufacturing process. The pressure transducers for example, were chosen because a sensor was needed that could contact the resin, be robust enough to hold up to repeated use and cleaning, and register pressures in the range from 0 - 12 psia. A summary of these basic criteria, the associated metric range and the actual equipment and specifications acquired are listed in Table 2.

Table 2: Summary of equipment used for this research.

Criteria	Metric Range	Equipment Used	Equipment Specifications
	13°C - 33°C	Endocal Refrigerating Recirculation bath	-20°C - 100°C
In-line Resin Flow Control, Easy cleaning	Low flow, ≤ .01 m/s	Compact Plastic Needle Valve, McMaster Carr	3/8" x 3/8" barbed ends, finely adjustable threads
Vacuum Pressure Control and Adjustability	0 - 6.5 psi	Alcatel Vacuum pump	25 Hp, Fully adjustable Vacuum Pressure
Record and Monitor Changing Mass for flow rate	Mass range: 0 - 2000g, Data output	Arlyns Scale	Mass: 0 -44 Kg, 5 Output Options Including Analog and USB Data logging
Record and Monitor Vacuum Pressure, Easily Cleaned	Pressure range: 0 - 12 psi, Data output, Minimal Resin Contact	Flush Mounted Pressure Transducers, Omega Engineering	Pressure Range: 0 - 100 Pisa, Analog Output, Sealed Flush Mount Sensor

Record and Monitor Resin & Glycol Temperature W/out cross contamination	Temp. Range: 13°C - 33°C, Data output	IR Thermometer	Temp. Range: -23°C - 871°C, Adjustable Emissivity, Analog Output, Laser Sight
Multifunctional Mold with Pressure Transducer ports	Accommodate Typical Laminate sizes	Milled Finish, T-6061 Aluminum Alloy	24" x 36" x 3/8" Al Plate, 3/8" Tapped NTP Ports for Pressure Sensors
Acquisition and Recording of Multiple Data streams	Up to 4 Channels	M Series Multifunction DAQ for USB - 16-Bit, National Instruments	Up to 80 Analog Inputs, USB Connection to Computer
Configurable Data Collection Software Application	Multi-Channel Acquisition, Data Manipulation	National Instruments LabVIEW Software	More Than 700 Math Functions, Graphical Programming

3.3. Test Procedures & Goals

The goal of this research based on a proposal to and funding by the DOE, was to investigate the manufacturing science associated with wind turbine blades. The manufacturing and testing conducted were designed to mimic typical practices used in the manufacture of wind turbine blades. Laminate quality being the metric by which the manufacturing process was to be assessed, a list of the primary factors contributing porosity were proposed. These factors are labeled "input parameters." Also of concern in the manufacturing process is the introduction of waviness either in the plane (IP) of the fabric or out of the plane of the fabric (OP). Since the wave flaws were determined to be caused primarily from mishandling or bunching of fabric, a distinction would be made from the porosity flaws in testing and flaw characterization.

3.3.1. The Taguchi Method and Input Parameters

The quality characteristic that is associated with manufacturing wind turbine blade composites with respect to porosity was determined to be "the smaller the better" [33]. Based on the Taguchi Design of Experiments for this quality characteristic, a list of manufacturing parameters i.e. input parameters were chosen that were most likely to affect the porosity content and, thereby, the quality of the laminate. Consideration was also given to the extent to which laboratory experimentation was going to be able to completely replicate the manufacturing conditions found in the industry. Factors, which could be controlled and replicated in the laboratory environment, were chosen and have been outlined in Table 3 along with their identifiers.

Table 3: Manufacturing parameters used to control variations in the manufacturing process.

Input Parameters	Parameter Identifier
Number Of Layers Of Flow Media	NFL
Laminate Architecture (Fabric Types)	FAA
Number Of Layers (Fabric)	NFA
Injection Flow Rate	IFR
Injection Temperature	ITS
Vacuum Pressure (Starting Pressure)	VPS
Degassed Resin	DGR

It is well known and clear to see form empirical data that some of these parameters are interrelated to which Darcy's law can be applied. In this relationship, seen in Equation 1, the resin flow velocity is directly proportional to differential pressure across the laminate. The permeability tensor, C_{ij}, can also be affected by the temperature of the flowing resin. These parameters were chosen initially based on empirical knowledge of best manufacturing practices but Darcy's law gives evidence to the validity of these choices.

$$v_i = -C_{ij}\left(\frac{\partial P}{\partial x_i}\right) \tag{1}$$

Each of these seven parameters could have a large range of variability; therefore, a range of parameter levels was chosen in order to indicate what low and high values were associated with that specific parameter. For parameters, such as number of layers of fabric or flow media, there are no standardized parameters for these values because laminate thickness is determined by the parts load requirements. This study was solely interested in highlighting the effects these parameters can have on laminate quality. Specific experiments were established to investigate the effects that variation in these seven parameters would have on laminate quality.

3.3.2. Test Matrix

A full, factorial study of the seven factors—layers of flow media, fabric type, layers of fabric, flow rate, injection temperature, starting vacuum pressure and degassed resin—and their associated high and low level settings was impractical since it would have required 128 test plates to be manufactured. This was cost and time prohibitive; consequently, a Taguchi Design of Experiments was conducted using Mathcad's built in design matrix tools. The purpose of this test design matrix was to reduce the number of tests that would be needed to be conducted, while still obtaining a test plan that could adequately analyze the effects of all the input parameters. Table 4 (see Appendix A for full, Mathcad documentation) shows the design matrix that was used to vary the specified parameters during testing.

Table 4: Taguchi Design of Experiments matrix which depicts the variations in each of the seven test parameters.

Run	NFL	FAA	NFA	IFR	ITS	VPS	DGR
1	1	Triax	2	low	low	low	no
2	1	Triax	2	high	high	high	yes
3	1	Uni	6	low	low	high	yes
4	1	Uni	6	high	high	low	no
5	3	Triax	6	low	high	low	yes
6	3	Triax	6	high	low	high	no
7	3	Uni	2	low	high	high	no
8	3	Uni	2	high	low	low	yes

The run numbers correspond to the 8 different laminates that would be manufactured. Associated with each of these run numbers were the corresponding parameter values. The high and low values for the parameters were determined based on extreme levels for each individual parameter. Table 5 shows the final test matrix for the various parameters with each of the associated high and low values.

Table 5: Test matrix used for manufacturing laminates.

Run #	Laminate #	Layers of fabric	Layers of flow media	Layup sequence	Resin temperature	Flow valve setting	Mold vacuum pressure	Degass resin
1	2315	2	1	Triax	13 C°	4-5 turns	6.5 psi	no
2	2316	2	1	Triax	33 C°	no valve	0 psi	yes
3	2317	6	1	Uni	13 C°	4-5 turns	0 psi	yes
4	2318	6	1	Uni	33 C°	no valve	6.5 psi	no
5	2319	6	3	Triax	33 C°	4-5 turns	6.5 psi	yes
6	2320	6	3	Triax	13 C°	no valve	0 psi	no
7	2321	2	3	Uni	33 C°	4-5 turns	0 psi	no
8	2322	2	3	Uni	13 C°	no valve	6.5 psi	yes

From each of the plates samples were cut to measure the porosity, fiber volume content, and ultimate strength in tension and compression. Porosity samples had to be taken from the plate in such a way so that the porosity at the gauge section of the ultimate strength samples could be measured as well as for the entire laminate. This required cutting one porosity sample from each side of the ultimate strength samples. Since three tension and three compression samples were cut out of each plate that meant there would need to be 7 porosity samples per laminate. Fiber volume samples were also cut out from three different locations around the laminate. Table 6 shows the sample test matrix with the corresponding number of samples per laminate.

Table 6: Test matrix of samples taken from each laminate.

Run #	Laminate #	Porosity samples	Tension samples	Compression samples	Fiber burn-off samples
1	2315	7	3	3	3
2	2316	7	3	3	3
3	2317	7	3	3	3
4	2318	7	3	3	3
5	2319	7	3	3	3
6	2320	7	3	3	3
7	2321	7	3	3	3
8	2322	7	3	3	3

3.3.3. Output Parameters

Since laminate quality was the primary metric by which the experimental plates were to be evaluated, it was logical that the percent of porosity in the laminates would be determined after the plates were manufactured. Two other important characteristics, which related to the quality of the laminate, were the fiber volume fraction and ultimately the failure strength. These factors, known as output parameters, were evaluated after the plates were manufactured and cured.

The porosity content was evaluated by analyzing micrographs produced using a Scanning Electron Microscope (SEM) pictured in Figure 41.

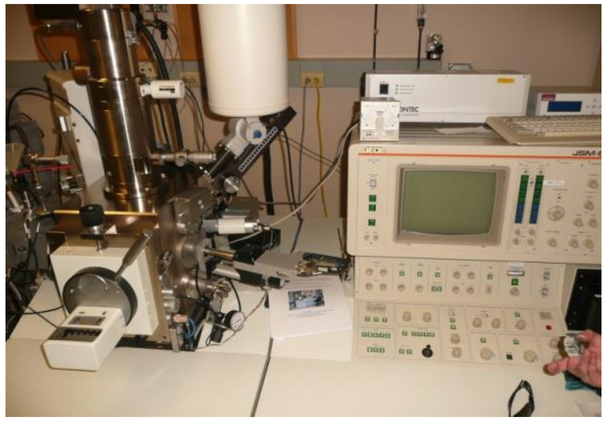

Figure 41: Scanning Electron Microscope (SEM) used for analyzing porosity samples.

From the images created using the SEM, a cross sectional average of void content was estimated. Through a series of steps such as cropping, despeckling, binarizing, and other such functions, the original micrograph was converted to a completely black and white image; the white pixels represented the void areas; the black pixels represented everything else. By comparing the black and white pixel count, an area fraction was determined which was proportional to porosity content. Image J, which is a free image processing application, Figure 42, was used to post-process the images and to create the binary pictures as seen in Figure 43. Using the macro utilities within Image J, code was developed to automate the time-intensive portions of the process. Using batch measurement techniques, area fractions would be measured for several files at once.

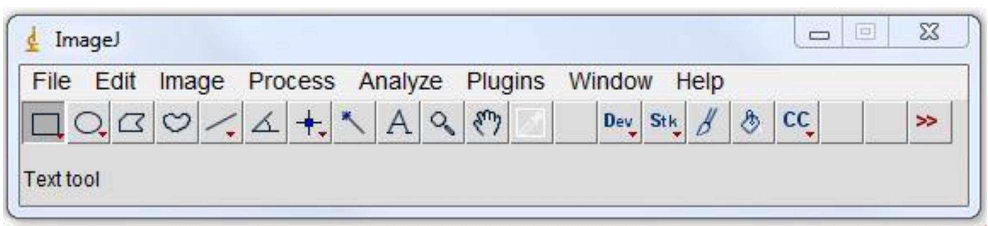

Figure 42: Image J user interface

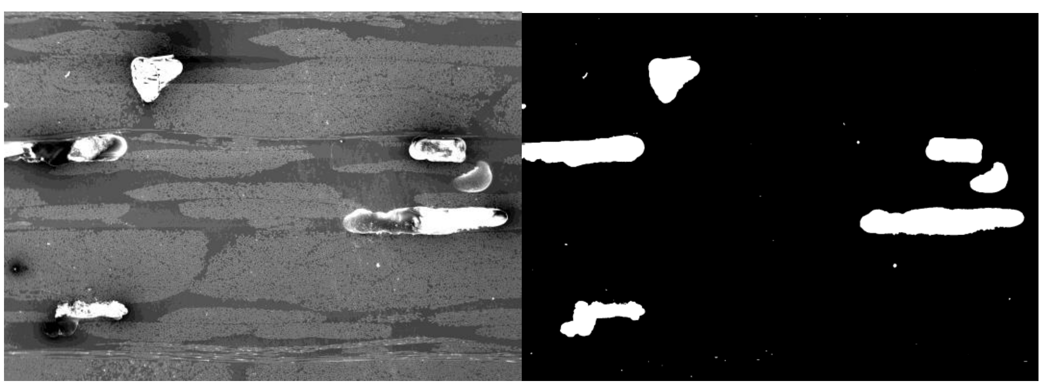

Figure 43: The left micrograph was created using the SEM; the right image is the binarized image.

Two sets of code were used to process the images. First the picture file was opened then the first macro was run which cropped the picture, converted it to 8-bit, and then saved it to a file. Second, the original file was opened again, and the second macro was run on the original picture. However, this time, in addition to the first two steps of the first macro, subtraction and multiplication operations were performed to remove a large portion of the noise in the picture and make the picture binary. Other functions such as "remove outliers" and "fill holes" were also applied to the processing steps. Finally, the code overlays the previous cropped picture, which enabled the operator to correct any missed or erroneous portions of the picture. The codes for these macros is included in Appendix D.

As was already stated, from these pictures an area fraction was calculated using "batch," a processing command, on several files at once. Later, using the estimated fiber volume fraction (FV%) of each laminate, the percent porosity by matrix was calculated using the ratio of black and white pixels. In Equation 2, the denominator is the number of pixels that represent the matrix of the laminate.

$$\frac{white\ pixels}{\left(black - \left((white\ pixels + black\ pixels) \times FV\%\right)\right)} = \%\ porosity \tag{2}$$

3.3.3.1. Fiber Volume Content

The second attribute of composite laminates to be evaluated was the fiber volume content. Fiber volume content has significance because it affects the weight of the structure and, also, the strength. Burn-off tests were performed to accurately compute the fiber volume fraction for each of the laminates. From each of the laminates that were manufactured, three 2 x 2-samples were cut to be used for the purpose of conducting the burn-off tests.

The samples were prepared by measuring all three dimensions to calculate the volume of the samples. Samples were then burned in an oven at 650 °C until all carbon based materials were completely volatilized. Figure 44 shows the oven used for these tests while it was in operation. All that was left, after the burn-off tests, were the silica fibers. When the silica fibers were weighed and divided by the glass density of 2550 Kg/m^3, the volume of glass fibers (V_S) for each sample was determined. The fiber volume fraction (V_F) was then computed by dividing the fiber volume (V_F) by the sample volume (V_S).

Figure 44: Burn-off test being performed in an electric oven at 650 ºC.

3.3.4. Manufacturing Method

As discussed previously the purpose of this study was to emulate industry standard practices for manufacturing wind turbine blade composites to better understand which aspects of the manufacturing process contribute the most to the flaws found in these composite laminates. An experimental setup was designed in order to construct laminates using the specified parameter settings that had been determined by using the Taguchi Design of Experiments method. Figure 45 shows the experiment setup which consists of the mold mounted on a wooden stand on the left, the heater/chiller and scale platform underneath, and the monitoring station on the cart next to it on the right.

Figure 45: Experimental setup of the mold, and all of the peripheral equipment, and monitoring station used in this study.

Once the laminates were manufactured, samples had to be prepared for the various tests. The tests to be made were determined based on the output parameters being monitored as discussed in the section, "Output Parameters." Additionally, tests were designed for the ultimate strength tests. In Figure 46 is plate number 2315, which corresponds to Run #1, labeled and ready for cutting.

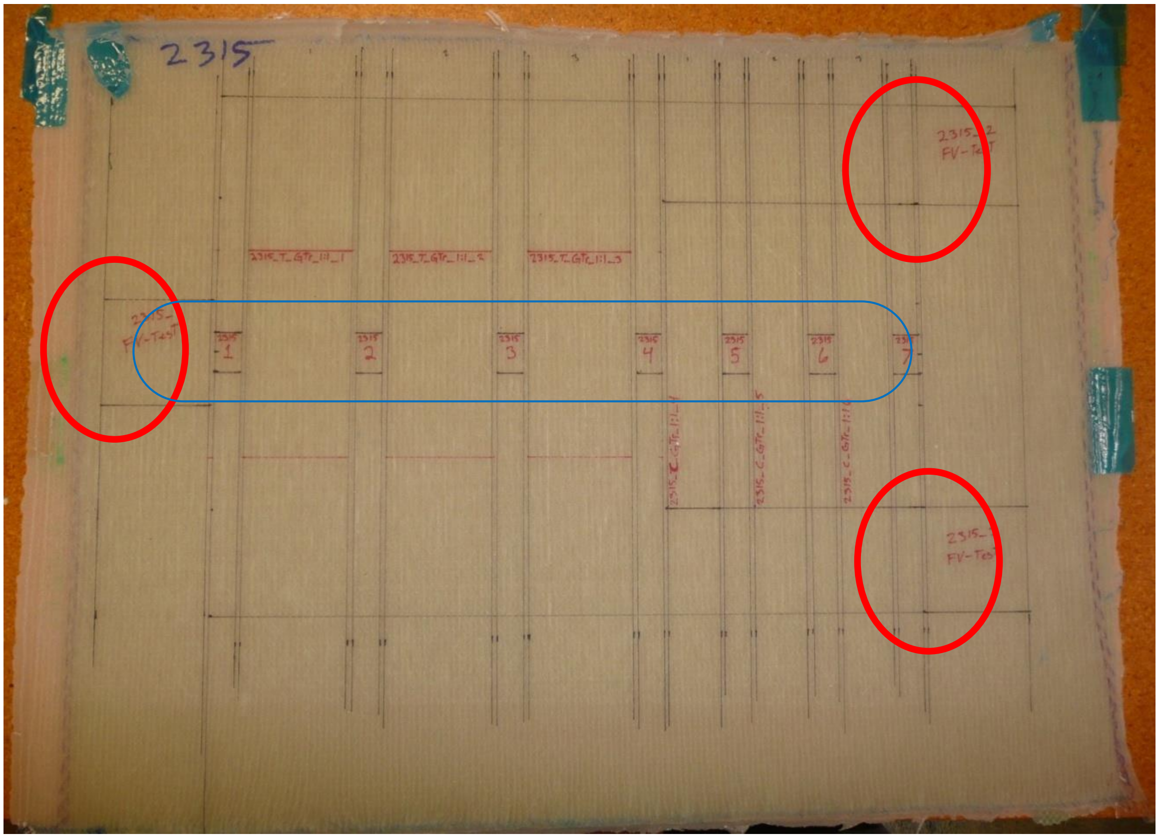

Figure 46: Laminate manufactured for Run # 1-- marked out for cutting out samples.

Three fiber volume fraction test samples (circled in red), seven SEM samples (circled in blue), three tension, and three compression samples were marked out for this plate. The fiber volume test samples were arranged around the plate to take into account any variability there might have been in the laminate itself. Fiber volume samples were measured in all three directions to be able to estimate the volume of the sample. Later these measurements were used with burn-off tests to calculate fiber volume fraction. The SEM samples were cut out in order to be able to estimate the porosity content at the center of the gauge section of the tension and compression samples. Each test sample would take the average of the porosity values calculated on either side of it. Once samples were cut, all of the test samples were measured, and the values for thickness and width at the center of the gauge section were recorded for stress calculations later.

4. EXPERIMENTAL RESULTS

The results of experimentation are presented in this chapter. The primary goal, to identify and quantify the effects of various processes that lead to the manufacturing flaws associated with composite laminates was achieved. Emphases will be placed on porosity flaws which are more common to MSU's composite group manufacturing process, but some results will show possible wave flaws associated with mishandling of fabric as well.

4.1. Process Parameter Test Results

The results of the parameter study associated with the introduction of porosity in laminates resulted in expected trends as well as some interesting correlations. First attention will be given to the process parameters that were that were monitored during the entire manufacturing process. Next the results of the burn-off test to calculate fiber volume fraction as well as the results of porosity measurements will be presented. Once all of the laminates had been manufactured, initial estimates of porosity were assigned to each of the laminates which appeared to have relatively even distribution of porosity. These initial estimates will be used to make correlations with each of the process parameters.

4.1.1. Resin Velocity Data

Resin velocity, being one of the main concerns with the vacuum infusion process, was monitored as discussed earlier using the Arlyns Scale. The reason for this is that resin has the propensity to initially travel very quickly through the flow media which can result in encapsulated fibers. The raw data from the scale, which can be seen in appendix C.1, was converted to laminate velocity by first taking the difference of two sequential mass values divided by two sequential time values, giving mass flow rate, and then dividing by resin density to result in a volumetric flow rate. The laminate thickness was then calculated based on the number of layers of fabric as well as the number of layers of flow media. The cross sectional area of the laminate could then be calculated using the thickness of the laminate and the laminate width of 20 inches, which when divided into the volumetric flow rate results in resin velocity through the laminate. Using the manufacturer's value for the neat resin density of 1.10 g/cm^3, and making the assumption that for these flows the resin is incompressible, Equation 3 represents the calculations used to report the flow rate.

$$\left(\frac{(Mass_{i+1} - Mass_i)}{(time_{i+1} - time_i)}\right) \times \frac{1}{\rho} \times \frac{1}{A_c} = V_R \tag{3}$$

In this equation resin density is represented typically as ρ, cross sectional area as A_c, and resin velocity as V_R.

From the results of this study it has been shown that indeed, laminate quality has considerable dependence on the rate at which resin is injected through the composite laminate. From initial estimates of porosity, correlations were made between the velocity of the resin and the amount of porosity in each of the laminates. It was shown that the laminates with the least amount of porosity also corresponded to those with low flow rates, Table 7. However the data does not completely correlate since there were multiple parameters being tested at once.

Table 7: Maximum velocity of the resin through the laminate.

Plate #	Max velocity (ft/s)	*Porosity*
2315	0.040	3%
2316	0.105	2%
2317	0.009	0%
2318	0.040	4%
2319	0.003	4%
2320	0.017	1%
2321	0.009	0%
2322	0.017	6%

4.1.2. Vacuum Pressure Data

The pressure sensors used in the mold for this study were a new idea which stemmed from the knowledge that correct vacuum pressure is important to laminate quality, but it was never fully explored. The data from the Labview program for these transducers was already converted to units of pressure so no additional data manipulation was necessary. One trend that was observed for the first time was that the max pressure differential between the inlet port and the outlet port was directly proportional to the initial vacuum pressure setting regardless of laminate configuration, infusion time, or any of the other parameters, Figure 47. This resulted from the fact that all of the laminates ultimately achieved approximately the same inlet pressure of just a little over 11 psi. This final inlet pressure was approximately 1 psi less than atmospheric pressure. The difference was determined to be the pressure of the resin in the injection line going to the resin bucket just a little above floor level.

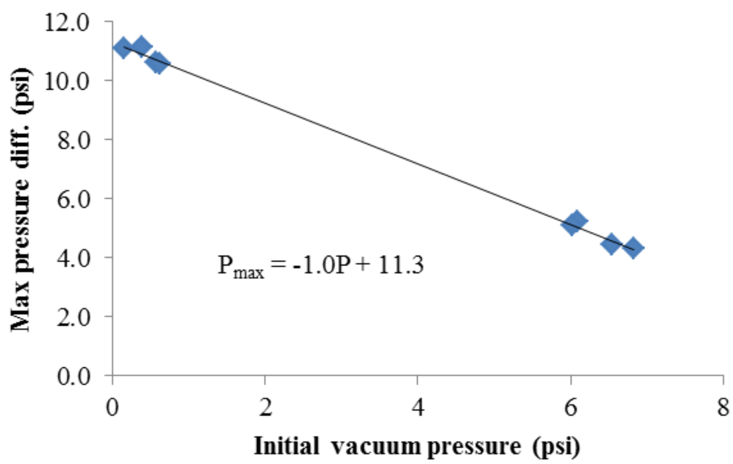

Figure 47: Correlation of maximum pressure difference and the initial laminate vacuum pressure.

Based on this direct correlation between the max differential vacuum pressure and initial vacuum pressure, it is expected then that max differential pressure should relate with estimated porosity similarly. In fact, the correlation was even more pronounced than that with flow rate. The data in Table 8 shows how almost exactly the pressure differential inversely matches the porosity content in each of the laminates.

Table 8: Maximum pressure differential between the inlet port and outlet port.

Plate #	Max pressure difference (psi)	*Porosity*
2315	4.3	3%
2316	11.2	2%
2317	10.6	0%
2318	4.4	4%
2319	4.3	4%
2320	10.6	1%
2321	11.1	0%
2322	5.1	6%

4.1.3. Resin Temperature Data

The resin temperature was monitored throughout the injection process using the infrared thermometer as a means of assuring that the resin temperature remained relatively constant. Due to the relationship between resin temperature and viscosity reported by the manufacturer in Figure 16, these temperature values translate to a known resin viscosity. The two average extreme values of temperature recorded in these data sets were 35°C and 13°C with approximate viscosity values of 180 mPas and 650 mPas respectively. From this data, average values of the temperature during the injection process were compared to the estimated porosity to discern if there was any correlation but none was found.

Table 9: The average temperature of the resin in the bucket during the infusion process.

Plate #	Average temperature (°C)	*Porosity*
2315	12	3%
2316	34	2%
2317	13	0%
2318	34	4%
2319	36	4%
2320	13	1%
2321	37	0%
2322	15	6%

The other three parameters that were controlled were also compared to the estimated porosity content. It was harder to make any correlations with these parameters as there did not seem to be any trend between them. The parameters for the number of layers of fabric (NFA) and laminate architecture (FAA) were included more as a means to understand the significance these factors have on the outcome of a laminate. In an actual manufacturing setting these parameters would only be varied as a means to satisfy the structural demands of the part. In Table 10 the estimated values of porosity are compared with the original input parameters.

Table 10: Controlled parameters compared to estimated porosity.

NFL	FAA	NFA	DGR	*Porosity*
1	Triax	2	no	3%
1	Triax	2	yes	2%
1	Uni	6	yes	0%
1	Uni	6	no	4%
3	Triax	6	yes	4%
3	Triax	6	no	1%
3	Uni	2	no	0%
3	Uni	2	yes	6%

4.1.4. Porosity and Fiber Volume Results

As discussed in the test procedures section porosity was measured by taking micrographs of representative samples from each of the eight plates and analyzing them for visible pores. Processing these pictures into black and white images is relatively simple since the porosity shows up white around the edges and often throughout the pores as seen in Figure 48.

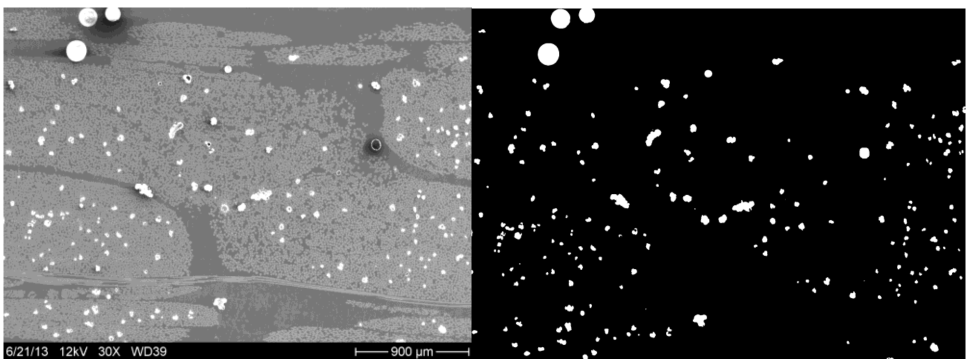

Figure 48: Micrograph of a sample from plate 2315 and its corresponding B & W image.

From these black and white images an area fraction is calculated which directly correlates to % porosity by laminate. The % porosity by matrix was also reported using (and the fiber volume values calculated from the burn off tests. The porosity values for all eight plates are presented in Table 11.

Table 11: Porosity values for each of the laminates manufactured.

Laminate #	*Porosity (laminate)*	*Porosity (matrix)*
2315	3.1%	6.0%
2316	1.8%	3.4%
2317	0.2%	0.5%
2318	3.5%	8.1%
2319	4.2%	6.7%
2320	1.0%	2.0%
2321	0.0%	0.0%
2322	6.3%	14.7%

Another interesting phenomenon associated with the porosity in the laminates is how well porosity was diffused throughout the laminates. The manner in which the SEM samples were cut out of the plates made it possible to investigate this because all the samples were cut from the plate in a line perpendicular to the resin flow. An investigation of this transverse laminate porosity profile shows that for most of the laminates porosity was very well diffused across the laminate, Figure 49. Only plate 2322 showed a large variability in the porosity profile. This large variability could be a result of the high porosity range that this plate exhibited. Possibly the mechanisms that induce these higher porosity values could have a higher level of uncertainty in dispersal characteristics. After comparing the images from the SEM analysis it is clear that plate 2322 had some very large channel voids as well as a large concentration of intra-tow voids. This is potentially an aliasing issue associated with this method of porosity measurement and the more variable dispersion of large channel voids.

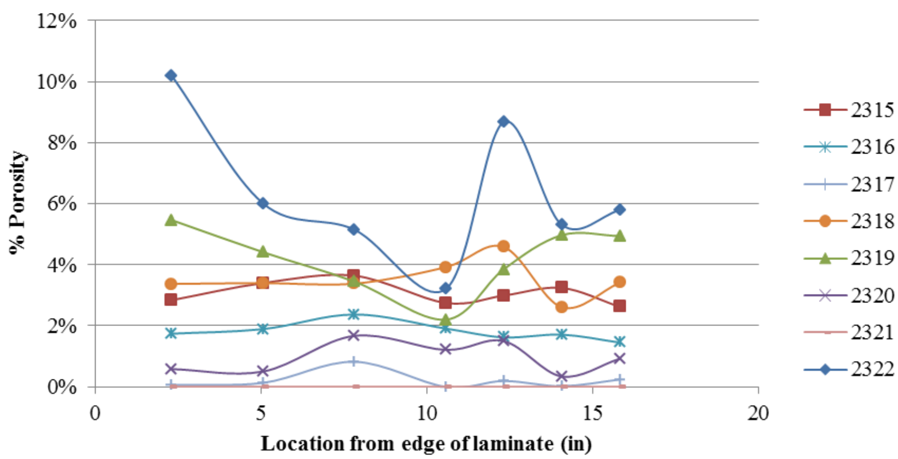

Figure 49: Porosity across the width of the laminate.

From the burn-off tests fiber volume results were calculated to provide correlations between the amount of porosity and fiber volume fraction. Most of the data seemed to follow general expected values except for the value associated with plate 2319. For some unknown reason the fiber volume of that laminate was particularly low, Figure 50.

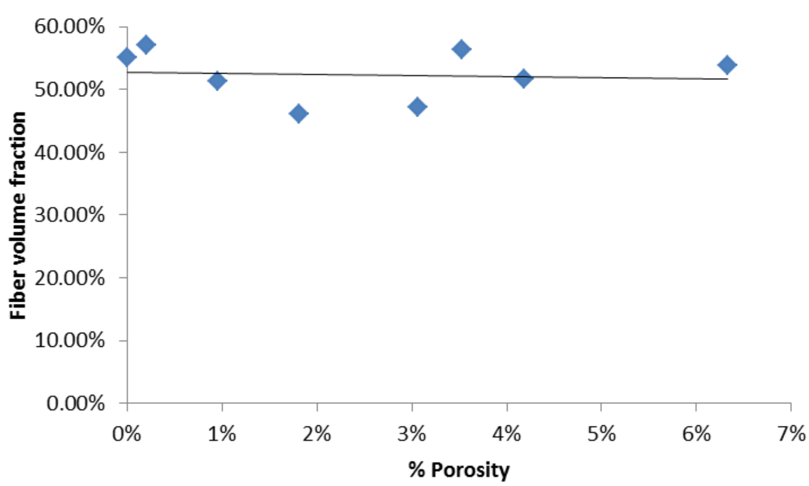

Figure 50: Fiber volume as a function of porosity.

4.2. Wave Flaw Results

Efforts were made to try and simulate the introduction of waves by mishandling the fabric during the lay-up process. Previous studies conducted by PhD students in the MSU composites group have concluded that waviness in composite laminates has a significant impact on laminate strength.

In an effort to validate qualitative knowledge of the processes that can result in wave flaws, several laminates were manufactured using the same techniques as those used in industry. An adhesive called Super 77 is commonly used in industry to hold layers of fabric in place during the lay-up process. The hypothesis was that this adhesive could be constraining the layers of fabric and thereby forming out of plane waves. The first laminate that was fabricated was a 20 layer uni-directional laminate wherein the second layer of fabric was adhered to the first with two out-of-plane waves. All subsequent layers were also adhered together with the adhesive before inserting it into the mold. Figure 51 shows the 20 layer laminate before it was inserted into the mold.

Figure 51: Out-of-plane waves inserted into 20 layers of uni-directional fabric using Super 77.

This laminate resulted in very small perturbations in fiber orientation that ultimately flattened out at the top of the laminate. However this process did prove the point that waves could be introduced in such a manor.

Likewise a thinner 4 layer laminate was constructed where only the first layer was perturbed and all the subsequent layers were adhered to that first layer. The amplitude and wavelength of the wave in this second laminate was also smaller and the angle steeper as compared to those of the first laminate. Figure 52 shows all four layers of the laminate stacked together with the wave inserted in all of the layers.

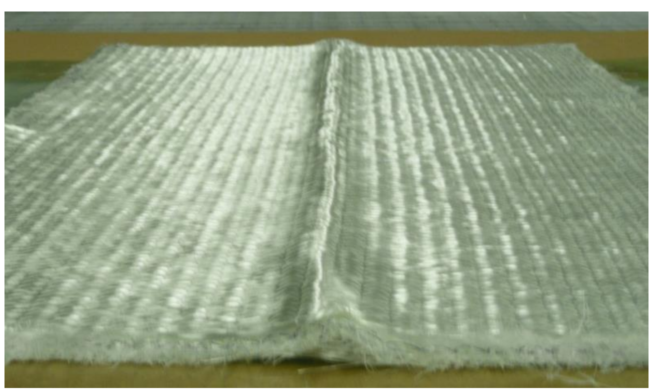

Figure 52: Laminate 2333 manufactured with a small amplitude and steep angle OP wave.

This laminate test plate resulted in a distinct wave in the cured laminate which proves to this concept for the introduction of waves.

4.3. Ultimate Strength Test Results

Samples were prepared and tested to compare ultimate strength with porosity content for each of the eight plates. Tension tests for the 2-layer laminates resulted in good test results however the 6 layer laminate samples were too thick to be broken in the gauge section. The only sample that broke was a result of a grip failure that crushed the laminate. Conversely, compression tests of the thicker 6 layer laminates resulted in good tests while the thinner laminates just buckled. Two of the 2-layer compression samples were prepared with strain gauges adhered to both sides and tested using shorter gauge lengths to see if positive results could be obtained. One uni-directional 2-layer sample was tested using an 18mm gauge length and one triax 2-layer sample was tested using a 37mm gauge length. Data from the 2-layer glass uni compression test in Figure 53 shows the obvious effects of buckling since the strain values from the two gauges diverge and gauge 1 begins to demonstrate tensile behavior. The 2-layer triax compression test shows similar behavior towards the end of the test except that for the first portion of the test the two strain gauges behave very similarly, Figure 54.

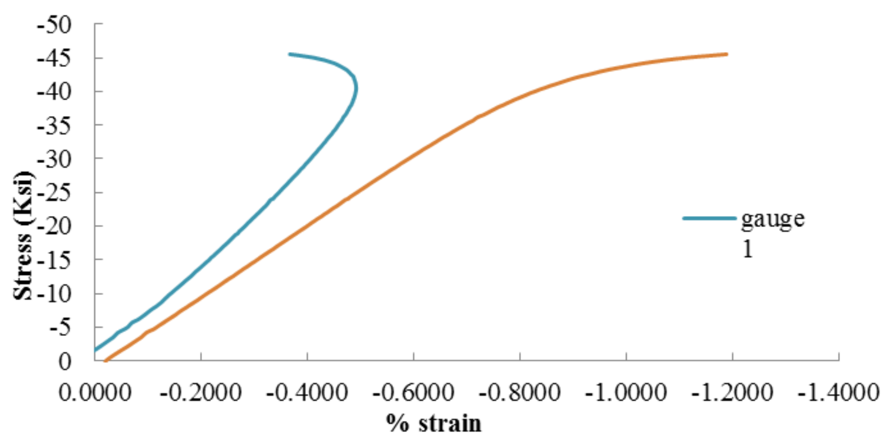

Figure 53: Compression test of 2-layer glass uni which shows buckling effects.

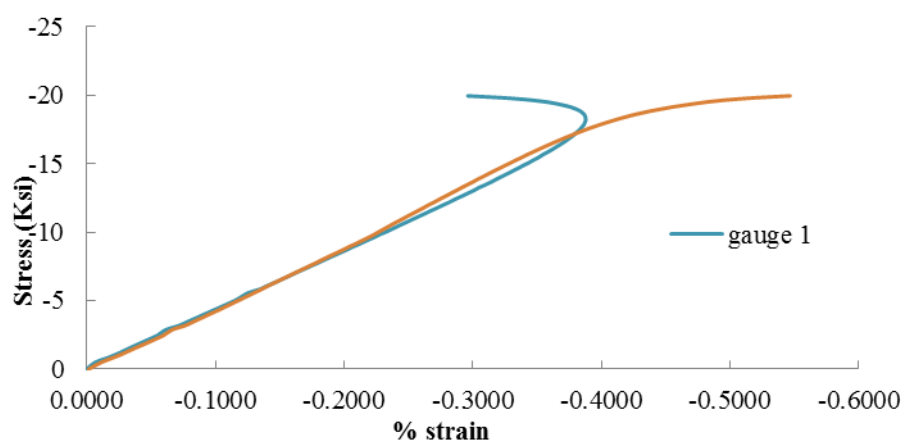

Figure 54: Compression test of 2-layer triax which shows buckling effects.

The strain gauged samples did not result in useful data so subsequent compression tests for the 2-layer samples were abandoned. For the 2-layer tension tests as well as the 6 layer compression tests, ultimate strength values were plotted against porosity and compared to values from tests conducted for the Effects of Defects study. These plots are contained in Figure 55 and Figure 56. In Figure 55 uni-directional laminate data is plotted for tension and compression. The Effects of Defects data are consistently low when compared to the data gathered for this study for the uni-directional laminates. This could be a scaling affect due to the difference in the number of layers of fabric. In the Effects of Defects study all laminates manufactured were four layers while for this study laminates were either 2 or 6 layers. Figure 56 shows the same data as Figure 55 except that it is for triax laminates. There appears to be significant discrepancy in the comparison of the triax data with the uni data. The one thing to note with all of these plots is that at least they seem to share the same relationship with respect to an increase in porosity. In other words the slope of the lines is relatively close between each similar data set.

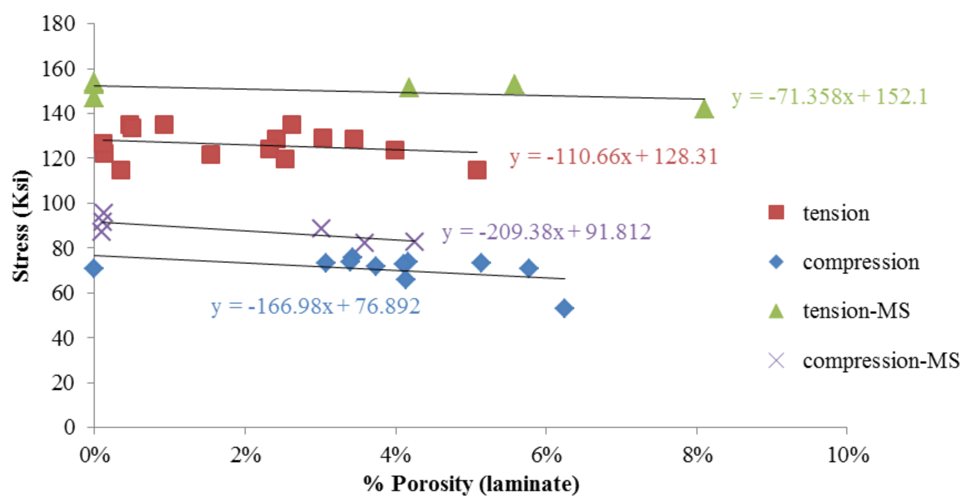

Figure 55: Ultimate strength comparison with porosity content for uni-directional laminates. Strength values were compared with samples manufactured for J. Nelson and T. Riddle.

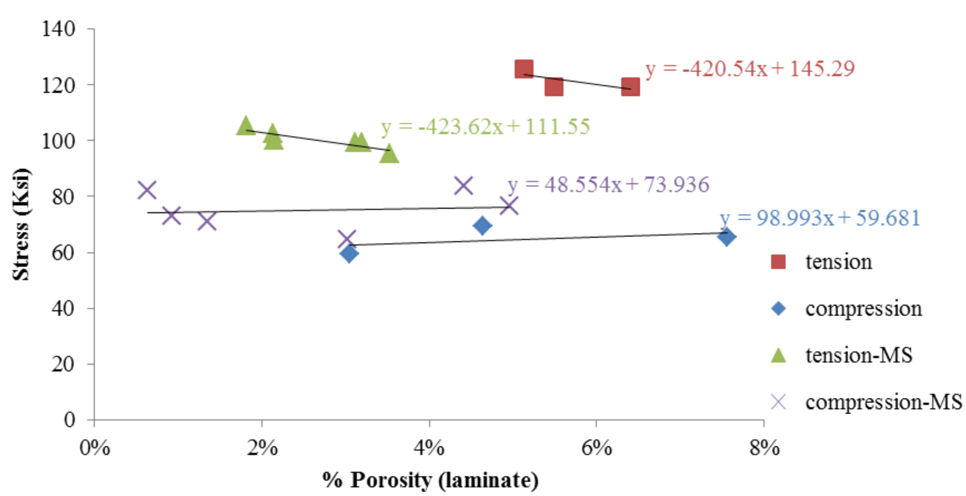

Figure 56: Ultimate strength comparison with porosity content for triax laminates. Strength values were compared with samples manufactured for J. Nelson and T. Riddle.

5. DISCUSSION AND ANALYSIS OF RESULTS

5.1. Analysis of Output Parameters

5.1.1. Porosity

From the porosity data gathered while studying the process parameters, it became apparent that some of the parameters correlate well with porosity and some did not. However it was not quite clear how significant any given parameter was so an Analysis of Variance Analysis (ANOVA) was conducted on the data using Mathcad's built in utilities. ANOVA employs statistical analysis techniques to analyze fractional factorial experimental designs and provide meaningful correlations between multidimensional data. One of the tools that ANOVA offers is a way to determine relative significance between such parametric data. For this research a significance plot was created by averaging the porosity values for both of the extreme levels of each parameter. For example, the VPS parameter was varied from the low value of around 6.5 psi to the high value of 0 psi. For each of the test laminates that were manufactured at a low VPS, the porosity content was averaged and compared to the averages at the high value. Equation 4 and Equation 5 show the two values that were calculated for each of the seven parameters. Once these two values were obtained a straight line was plotted in between them.

$$VPS_- = \frac{1}{4}\left[\sum_{i=1}^{4}(VPS_{low})_i\right] \tag{4}$$

$$VPS_+ = \frac{1}{4}\left[\sum_{i=1}^{4}(VPS_{high})_i\right] \tag{5}$$

In these equations VPS_- is the average porosity of the individual laminates where the vacuum pressure was at a low value, and VPS_{low} is the associated porosity value for each laminate. Similarly VPS_+ is the average porosity for the high vacuum pressure setting which resulted in laminate porosity values of VPS_{high}. Each of the parameters was analyzed in the same way and Figure 57 displays this data for all seven parameters and clearly shows the dominant trends.

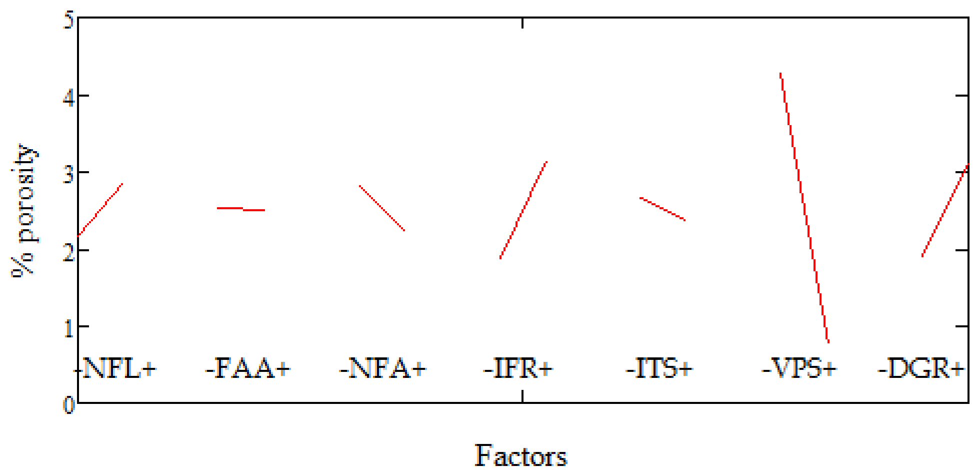

Figure 57: ANOVA plot of the significance of the different process parameters with respect to porosity.

The most interesting fact that has been produced from this research is that the injection flow rate is not the predominant factor in the manufacturing process as was previously thought. As seen in the ANOVA plot, the vacuum pressure is the primary factor which dictates how much porosity will result in a laminate. From this data it is apparent that the vacuum pressure in the mold is the most critical aspect of the manufacturing process in terms of minimizing porosity. Maximizing the vacuum pressure then results in the lowest levels of porosity and, thereby, a higher quality laminate. The injection flow rate follows vacuum pressure in terms of significance but is surprisingly not drastically more significant than some of the other parameters. This information also points out a new method for producing porosity in laminates for strength correlation.

Part of the BRC Effects of Defects study was aimed at characterizing porosity flaws by comparing porosity content to ultimate failure strength. Several different methods of introducing porosity in laminates were considered and tested with varying success. The results of this research have introduced a new method for more accurately predicting and controlling void formation in composite fiber laminates. Figure 58 shows the correlation of porosity with initial vacuum pressure.

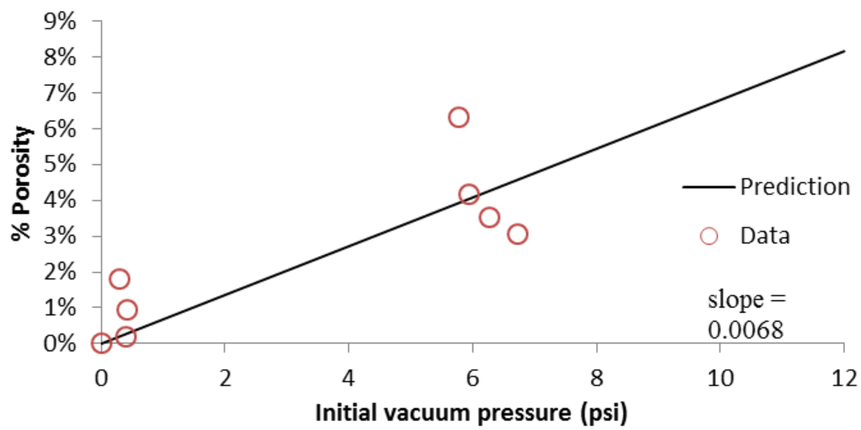

Figure 58: Porosity as a function of initial vacuum pressure.

The general trend depicted in Figure 58 shows that by controlling the initial vacuum pressure, porosity content in a laminate could potentially be controlled very accurately.

5.1.2. Fiber Volume Fraction

Another important aspect of laminate quality, and consequently considered as one of the output parameters, is the fiber volume fraction. Fiber volume fraction is the amount of reinforcing fiber material contained in a given volume of a composite. Research has shown that an increase in fiber volume fraction can reduce the overall weight of a composite laminate and in some cases even increase the strength as well, [34-36]. For these reasons, fiber volume fraction was chosen as one of the output parameters for the manufacturing process of composite laminates to investigate the effects of the input parameters. Samples that were prepared for the fiber volume measurement were burned according to the procedures outlined in the Experimental Setup & Process Modeling chapter. Initial burn-off tests performed were not done correctly and did not result in complete combustion of all the matrix material in the samples. This resulted in a substantial amount of residue left on the burned samples. It was unclear how much this residue effected the results; therefore, subsequent samples were burned to the same point, weighed, and then they were completely burned and weighed again. The error in the values between six different samples was less than 2%; thus, the residue that had been left on the initial samples seemed to be acceptable. Figure 59 shows the difference in appearance between samples that were burned adequately (right) and those that were not (left).

Figure 59: Fiber volume samples that were not burned off completely (left), and samples that were completely burned (right).

Fiber volume fraction values calculated through burn-off tests were validated by comparing them to fiber volume estimated from the thickness of the laminate. The experimental values agree substantially with estimated values. The comparison can be seen in Figure 60.

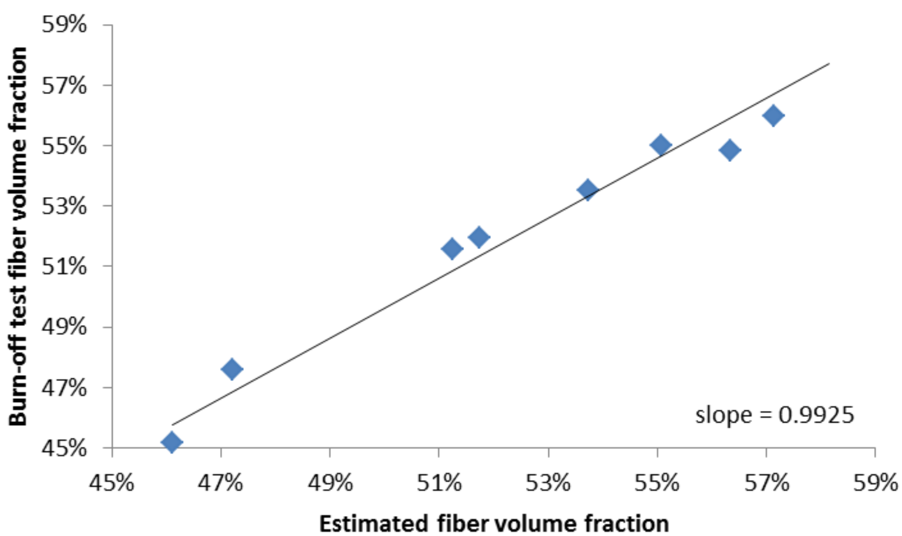

Figure 60: Comparison of measured and estimated fiber volume fraction.

Once the values for the fiber volume tests were verified, an ANOVA analysis was performed to determine which of the process parameters might have the most significant effect on the fiber volume fraction. In Figure 61, it is clear to see that the laminate architecture has the largest effect on fiber volume fraction. This is likely due to the fact that ±45 degree fiber bundles don’t seat in between the bundles of the zero degree fabric, and, therefore, result in a substantial increase in channel sizes between fiber bundles. These larger channels would fill with resin resulting in more matrix material in the laminate, thus, a lower fiber volume. This prediction agrees with the trend seen in Figure 61 which shows that the triax laminates resulted in a lower average fiber volume fraction.

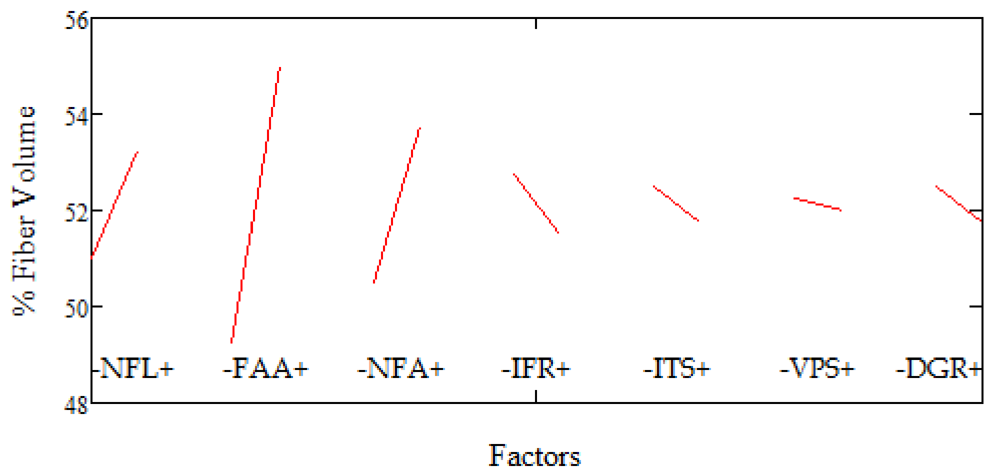

Figure 61: ANOVA plot of the significance of the different process parameters with respect to fiber volume fraction.

An interesting, yet expected result to note about the analysis of the fiber volume fraction is the correlation with initial vacuum pressure. Whereas porosity was largely affected by the vacuum pressure, the fiber volume fraction is not. This is because the fiber volume fraction of the laminate would be affected more by the final vacuum pressure then by the initial. For these tests, the final vacuum pressure was relatively constant for all eight runs. This is largely an artifact of the specific manufacturing process used in the composite group's lab at MSU.

5.2. Modeling

One of the primary goals of this project was to create a means of predicting laminate quality based on manufacturing process parameter settings. Two models were developed to be used to educate or inform composite laminate technicians. Through a series of quantitative investigations into the manufacturing process a numerical model using MathCad was created. In addition, a qualitative approach was used to create the second model. The different types of flaws and their associated methods of introduction dictated the use of a causal model approach to analyze the flaws rather than a more traditional empirical model. The second section will focus on the development of the causal model using a tool known as an expert system.

5.2.1. Model of Output Parameters

Based on the data gathered in this research, models were created to predict the porosity content and fiber volume fraction in a laminate based on the settings of the input parameters. The model fits the results of either porosity content or fiber volume fraction to the input data generated by the design matrix. MathCad's "polyfit" command was used to generate a multivariate, polynomial regression surface. Once this multi-dimensional surface was created, it could be called in with new input parameter values to make predictions of outcome. Figure 62 shows a screen shot of the code used to produce the model.

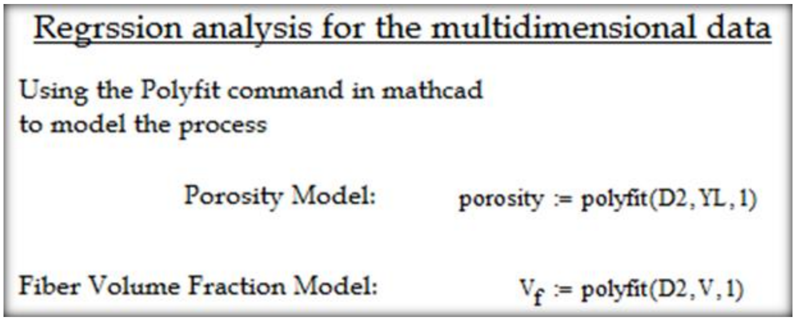

Figure 62: MathCad polyfit command used for modeling outcome of composite laminates.

The model utilizes the original design matrix, which was calculated using the Taguchi Method (matrix D2), and fits it against the output data collected (porosity data is YL, and fiber volume data is V). For any given parameter, there are only two data points, a maximum and a minimum; therefore, a first order polynomial equation was used to fit the data. As an example, if there were two factors, or in our case process parameters "A" and "B," and a possible interaction between them "AB," then the multivariate polynomial regression fitting equation would have the form of Equation 6.

$$Y = c_0 + c_1 A + c_2 B + c_3 AB \tag{6}$$

The "c" coefficients are the individual regression fit coefficients associated with each of the parameters. MathCad determines these coefficient terms using a linear least squares analysis. The least squares function, Equation 7, can be minimized by taking the derivative with respect to the matrix of "c" coefficients and setting it equal to zero. The matrix [A] is composed of the input parameter values and the [**Y**] matrix consists of the output values.

$$S(\boldsymbol{c}) = \| [\boldsymbol{A}][\boldsymbol{c}] - [\boldsymbol{Y}] \|^2 \tag{7}$$

The term c_0 would be considered the intercept value and all of them were determined by using the polyfit command; in the case of the porosity and fiber volume models, there were 7 factors. The original settings for the eight runs were individually fed into the model to verify that the output could be predicted. Indeed the actual output values were verified. In Figure 63 the model was used to predict the individual outcomes of the initial eight laminates. A similar investigation was done for the fiber volume fraction and the data for that can be found in Appendix E.

Validation of porosity results using model:

Prediction of parameters from run 1:	$porosity\left(In^{\langle 1\rangle}\right) = 3.1$	Actual value = 3.1%
Prediction of parameters from run 2:	$porosity\left(In^{\langle 2\rangle}\right) = 1.8$	Actual value = 1.8%
Prediction of parameters from run 3:	$porosity\left(In^{\langle 3\rangle}\right) = 0.2$	Actual value = 0.2%
Prediction of parameters from run 4:	$porosity\left(In^{\langle 4\rangle}\right) = 3.5$	Actual value = 3.5%
Prediction of parameters from run 5:	$porosity\left(In^{\langle 5\rangle}\right) = 4.2$	Actual value = 4.2%
Prediction of parameters from run 6:	$porosity\left(In^{\langle 6\rangle}\right) = 1$	Actual value = 1%
Prediction of parameters from run 7:	$porosity\left(In^{\langle 7\rangle}\right) = 0$	Actual value = 0%
Prediction of parameters from run 8:	$porosity\left(In^{\langle 8\rangle}\right) = 6.3$	Actual value = 6.3%

Figure 63: Confirmation of initial porosity values using the model.

The model was able to predict the initial outcomes very accurately which would be expected. However, what was needed was to verify that the model would be able to predict one of these output parameters if the inputs parameters were varied from those used to create the model.

In order to determine the quality of the model created, two additional laminate plates were manufactured using an alternate variation of each of the seven input parameters. The parameter settings for the two plates, 2345 and 2346 are shown in Table 12.

Table 12: Input parameters for the two validation plates.

	Plate 2345	Plate 2346
Number Of Layers Of Flow Media	1	2
Laminate Architecture (Fabric Types)	1	3
Number Of Layers (Fabric)	8	4
Injection Flow Rate	.03	.03
Injection Temperature	22	22
Vacuum Pressure (Starting Pressure)	3.2	0.5
Degassed Resin	1	0

The results of these tests show relatively strong agreement with the model. Figure 64 shows the output of the model based on the initial settings of the input parameters and compares these results with the actual values. In plate 2345, the porosity predicted was 1.82%; the actual porosity measured 1.87%. The difference between the predicted porosity and the measured porosity was only .05%. The model successfully predicted the porosity of the second plate as well.

$$\text{plate 2345} \qquad \text{porosity}\left(\begin{pmatrix} 1 \\ 1 \\ 8 \\ .03 \\ 22 \\ 3.2 \\ 1 \end{pmatrix}\right) = 1.82 \qquad \text{Actual value} = 1.87\%$$

$$\text{plate 2346} \qquad \text{porosity}\left(\begin{pmatrix} 2 \\ 3 \\ 4 \\ .03 \\ 22 \\ 0.5 \\ 0 \end{pmatrix}\right) = 0.09 \qquad \text{Actual value} = 0.06\%$$

Figure 64: Results of the validation test plates.

5.2.2. Expert System Model for Diagnosing Laminate Flaws

The process of implementing a qualitative model, such as an expert system, requires a firm understanding of the entire process of manufacturing composite laminates. This model was designed to be used as a diagnostic tool for troubleshooting flaws found in glass fiber composite laminates similar to those manufactured in the wind turbine blade industry. The first step for building this model involved establishing a "laminate time line" or a procedural outline which categorizes the different phases of the process and the associated types of flaws that are typically introduced in each phase. A further classification groups the different flaw sources into one of the following categories: Porosity formed by leaks, Porosity formed by process, and Wave flaws. Figure 65 shows the work flow chart which breaks the manufacturing process into the five main stages, Material Preparation, Lay-up Laminate, Infuse Laminate, Mold Cure, and Post Cure. It is interesting to note that there are far fewer instances where wave flaws can be introduced into a laminate then porosity. Also the types of flaws being studied here are only affected by conditions occurring in the first three stages of this process. Flaws that are introduced during the mold cure or post cure processes have more to do with the chemical interactions of the resin system and are not considered significant to the introduction of porosity.

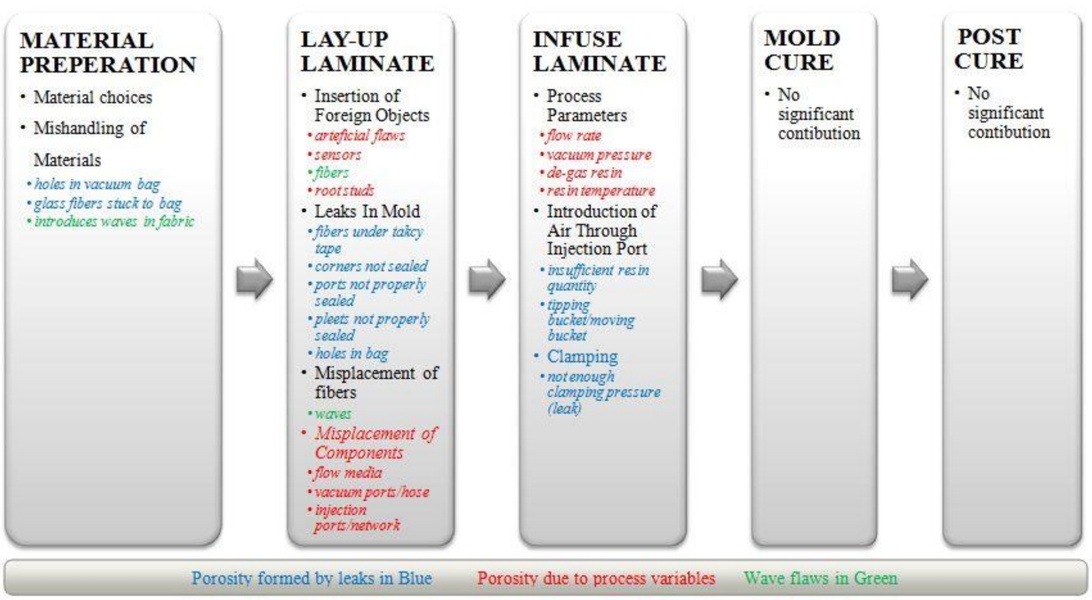

Figure 65: Laminate work flow and flaw introduction model.

This work phase flow chart does not account for the effects that 3-dimensional molds have on the outcome of porosity. More complicated geometries will affect the resin flow and, therefore, porosity content in the laminate. Wave flaws also become a prime consideration with more complicated geometries. As more curved surfaces and corners are introduced into the mold and part design wave flaws can be caused by fabric being bunched. This factor could potentially greatly increase the complexity of this model and was not considered here. Further investigation into complex geometry dependence would be beneficial for a complete development of this model.

The next step in the process of creating the expert system model was to develop a questioning hierarchy which would work backward from a flawed laminate and isolate which source caused the flaw to occur. This hierarchal list is important for creating questioning that leads an operator to a specific outcome. Figure 66 shows the basic outline of questioning used for the model.

Finally questions was developed based on extensive manufacturing experience, that would potentially direct a composite laminate technician through a series of backward chaining rules from one level to the next.

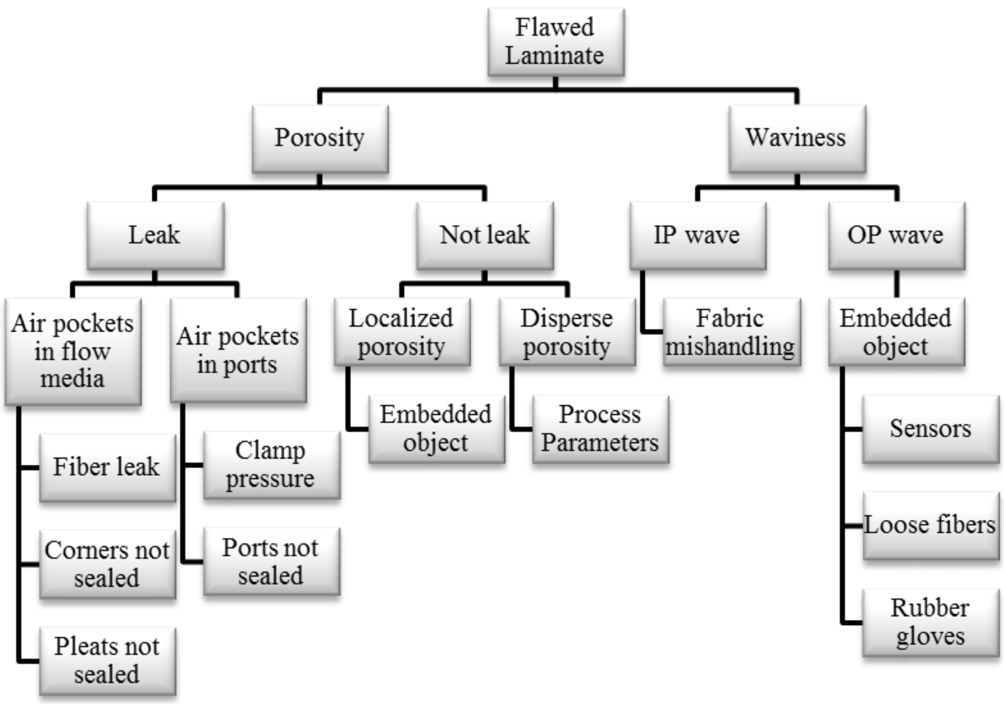

Figure 66: Questioning hierarchy for development of an expert system.

There are several different software applications for developing an expert system. Some applications utilize internet-based object oriented programming for expert system development while other software applications require minimal programming to execute logical commands. A program known as CLIPS (C Language Integrated Production System), was used for this research. CLIPS is a free expert system development software package which can be downloaded online. CLIPS was designed so that it could be fully integrated with other languages allowing a programmer to utilize tools for creating Windows-based Graphical User Interfaces thus increasing the utility of this tool. For the purposes of demonstrating an expert systems application to the composite manufacturing process, ten questions and their associated rules were programmed using the CLIPS interface. All of the questions for this program were developed to be answered with a “yes” or “no” answer. The expert system was then initiated using the dialog window of the CLIPS software. The file was loaded, reset, and then run which begins the questioning. The code used for this model is contained in APPENDIX F. Figure 67 shows some of the questioning that results from executing the program.

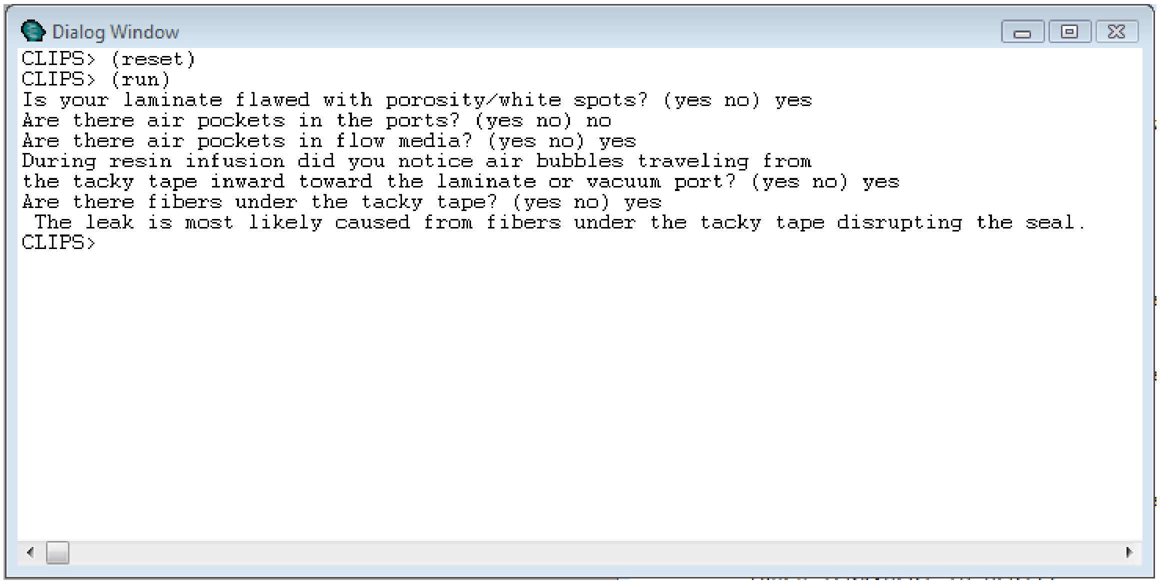

Figure 67: CLIPS dialog window showing some of the backward chaining questioning that results from this tool.

5.3. Observations

5.3.1. Porosity Formation

According research described in R. K. Roy's [28] work, one of the mechanisms for void formation occurs when resin flow is too slow. If the flow is too slow, such as when the pressure gradient is not sufficiently large, resin will flow faster through the fiber bundles than through the channels due to capillary action and potentially encapsulate air pockets in between the fiber bundles. Conversely, if the flow is too fast, resin flow through the larger channels in between the fiber bundles can overtake the flow through the bundles and create dry spots inside the bundles[32]. This has been verified through the current study and can be seen in Figure 68 and Figure 69.

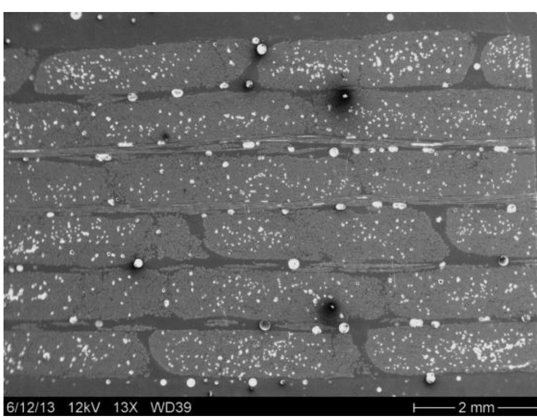

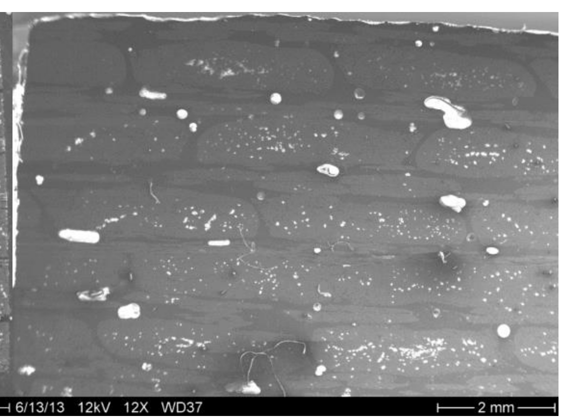

Figure 68: Micrograph of a laminate infused with a high flow rate.

Figure 69: Micrograph of a laminate infused with a low flow rate.

The laminate designated as plate-2318, pictured in Figure 68, is the result of high flow rate. Porosity can be seen as the white spots, and it is clear to see that there is more porosity inside the tows than there is in Figure 69, plate-2319. Clearly, the voids that appear in between the fiber bundles in Figure 68 are smaller than those in Figure 69. Both of these laminates were infused at a low vacuum pressure.

5.3.2. Mold Pressure Equalization

The pressure sensors used in the mold provided a unique insight into processing effects related to vacuum leaks. As a result of atmospheric pressure bleeding into the mold at one of the transducers more than the other, the pressure at the ends of the mold did not tend to equalize during the curing process. This unequal pressure distribution can occur for example when one of the ports is not sealed adequately as seen in Figure 70. Other leaked plates have shown that both of the sensors simultaneously achieve atmospheric pressure which would indicate that both of the sensors were experiencing an equal amount of vacuum leak. Leak severity is the determining factor for how much porosity will result in a laminate and the extent to which it will spread throughout the laminate. Leak severity can be quantified by examining the leak rate or the rate of equalization to atmospheric pressure that a laminate will reach while under vacuum. Theoretically, there would be a critical leak rate that would not yield any visible porosity in the laminate, a value which would likely be process dependent. Quantifying this critical leak rate value would need to be conducted for each specific mold process and would depend on a variety of factors including the type of leak, the materials used to build up the bagging process, and run distance for the leak.

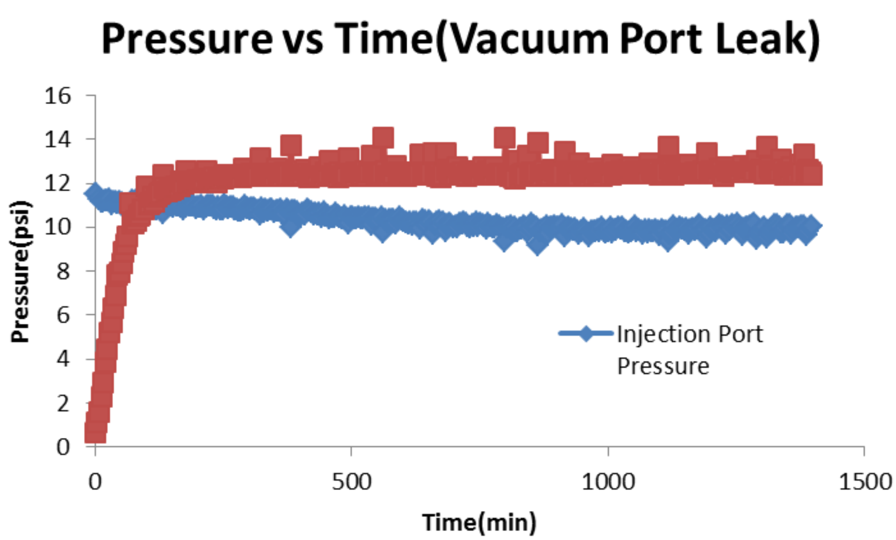

Figure 70: Pressure values at inlet and outlet ports of the mold during cure while vacuum port is leaked.

For laminates that were manufactured without any leaks, mold pressure was observed to equalize between 9 - 10 psi. This result occurred regardless of initial vacuum pressure, sparking curiosity, which led to another realization. The pressure at the injection port seemed to always reach 11 psi and then it would plateau, again regardless of initial vacuum pressure. Consequently, the pressure difference of this maximum inlet pressure and atmospheric pressure of around 12 psi was assumed to be the result of the pressure due to gravity on the volume of resin in the injection tubing. Using Bernoulli's pressure equation below, it was verified that the weight of the resin in the injection tube was the cause for the consistent max inlet pressures.

$$P = P_0 + \frac{1}{2}\rho V^2 + \rho g h \tag{8}$$

In Equation 8, P is the pressure at the inlet sensor, the static term P_0 is atmospheric pressure outside the mold, and the potential term includes resin density ρ, acceleration due to gravity g, and h the height of the mold surface above the resin bucket. The dynamic portion including the velocity term V, of this equation is neglected since the resin is at rest for the period of time that under consideration. Since the acceleration term of this equation is acting in the downward direction, the resultant pressure is also acting downward in opposition to the pressure gradient between atmospheric pressure outside the mold and vacuum pressure at the inlet to the mold. Figure 71 shows the experimental setup of the resin in the bucket on the scale at approximately 25 inches below the surface of the mold.

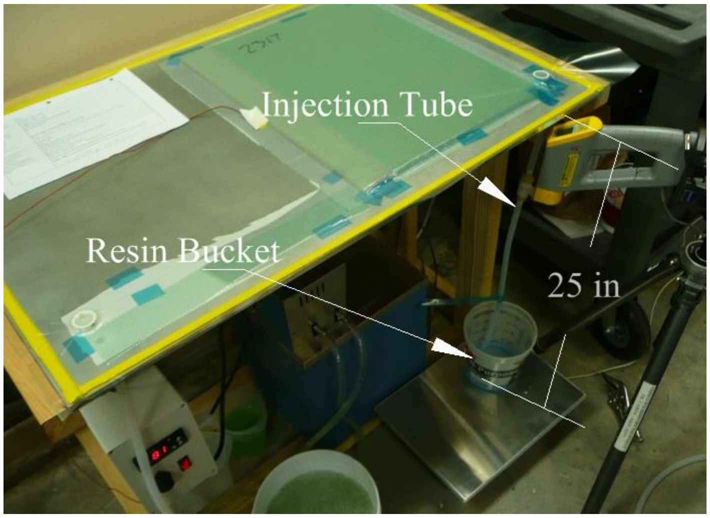

Figure 71: Laminate manufacturing setup with mold surface about 25 inches above resin bucket.

5.3.3. Pressure Spikes During Infusion

During the process of infusion, three of the laminates showed a spike in the output pressure data. This phenomenon seemed significant enough to investigate since it occurred in three of the laminates that were manufactured. Figure 72 shows a representative plot of the output pressure readings from plate 2318. Plates 2317 and 2319 also displayed similar events in the pressure data.

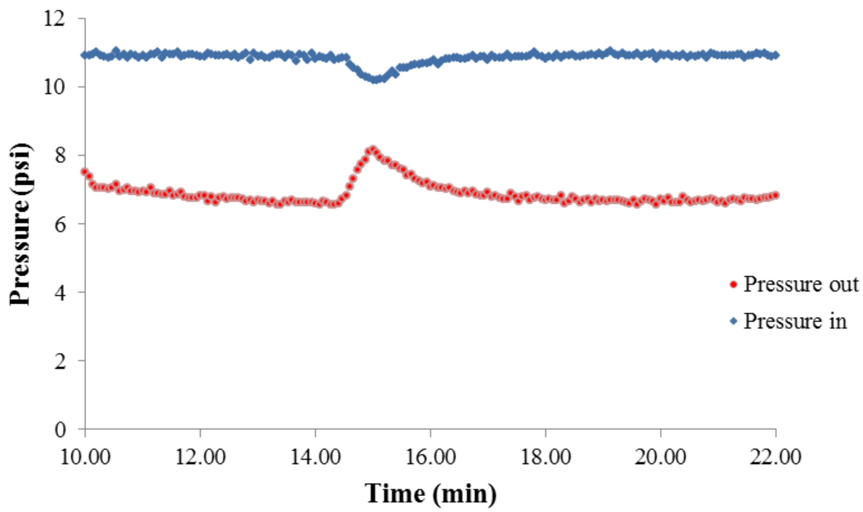

Figure 72: Spike in mold pressure for plate 2318.

The interesting thing to note in the response of the event is that in all cases the output, or vacuum port transducer registers an increase while the input or injection port transducer registers a decrease in pressure. This seemed to rule out the possibility that it could be caused by a momentary spike in the excitation voltage for the transducers; however this conclusion was verified in testing. In hopes that there could have been some kind of visual cue to the events, video footage for plate 2319 was analyzed. Video was not captured for the other two plates; however this video showed that for the time that the event occurred the flow front had just reached the end of the flow media only a few seconds before. This also seemed to be an unlikely cause since all of the laminates where configured the same way in terms of the use of flow media. Ten other laminates that were subsequently manufactured using the same system. Only one of these laminates showed a similar event, but again the cause was undetermined. It is assumed that the cause of these events were associated with an anomalous short between the signals in the Daq hardware.

6. CONCLUSIONS AND RECOMMENDATIONS

The objectives for this research were obtained through a series of quantitative and qualitative evaluations of the manufacturing process for wind turbine blade composite laminates. The 3 main contributions of this research and their benefits to industry are:

- Implementation of new instrumentation and process monitoring techniques to improve manufacturing process control and monitoring.
- Development and validation of an empirical model for the manufacturing process parameters.
- Development of a basic expert system model to diagnose flawed laminates through a series of backward chaining inference rules.

First of all, this research has sought to impact industry practices by improving current manufacturing techniques. The most obvious implication of this research is in the area of instrumentation. Using the instrumentation techniques developed for this research would improve process monitoring and control and, consequently, product quality. These instruments could be easily integrated into current manufacturing processes especially utilizing various mold pressure sensors to monitor vacuum pressure.

The second contribution to the understanding of blade manufacturing made by this research is to show the significance of effect of process parameters on laminate quality. Injection flow rate (IFR) was one of the input parameters considered in this study. Laminate quality has considerable dependence on IFR. This research revealed a significant correlation, the 2nd highest level of significance, between the resin velocity and porosity. However, IFR showed even greater significance of effect on fiber volume fraction. Although IFR was once again the 2nd highest factor, it was somewhat more of a factor in fiber volume fraction than porosity. Of the seven in-put parameters considered, injection flow rate is the most consistent in its effect on laminate quality.

On the other hand, vacuum pressure i.e. starting pressure (VPS) is inconsistent in its effect on the two out-put parameters. VPS had the highest significance of effect on porosity but no significant effect on fiber volume fraction. Fiber volume fraction out-put parameter would naturally show more dependence on VPS if the vacuum pressure differential could have been varied more substantially by changing the experimental setup.

Laminate architecture (FAA) had no significant effect on porosity but the highest effect of the parameters on fiber volume fraction. The number of layers of fabric (NFA) contributed more to the fiber volume fraction than porosity. However, as noted previously, FAA and NFA would only be varied as a means to satisfy the structural demands of the part being manufactured.

The number of layers of flow media (NFL) had about the third most significance of effect of the seven parameters on both porosity and fiber volume fraction with only slightly more effect on fiber volume fraction. While it would make sense that this parameter would not have as great an effect as some of the others, it is unclear why it has the effect on fiber volume fraction that it does.

The results show that the resin temperature (ITS) trended the right way but its overall effect on laminate quality was rather low. This was surprising because the resin temperature is directly related to the viscosity of the resin. The likely cause of this phenomenon is that the resin temperature was equalizing very rapidly as it entered the mold.

No reliable conclusions can be drawn regarding degassed resin (DGR) because the results achieved were inconsistent with expected results based on past experience. Thus, further investigation is required in order to better analyze the degree of significance of this parameter.

By using the methods developed in this research for identifying multiple process parameters and ranking their significance, key factors could be identified which would contribute to product quality. It was shown and validated that numerical modeling could be established which would allow technicians to target specific process parameter values and, thereby, decrease scrap rates. Also, previous research was verified which differentiated the two types of porosity in laminates and the triggers for their formation. Pictures produced using the SEM show that channel void formation is dominant when resin flow velocity is low while the converse was also noted which shows a higher concentration of tow voids for laminates with high flow rate.

Finally, the implementation of an expert system model of the blade manufacturing process can be used by industry to train new technicians and provide a means of capturing heuristic knowledge from expert employees. This expert system model could also be used to diagnose flaws.

Some of the limitations of this research were the breadth of fabric architectures tested, laminate and mold configurations, and the types of flaws that could be introduced with respect to the given experimental setup. Time also limited the number of laminates that could be manufactured which is why the Taguchi Design of Experiments was implemented to create a data set that would adequately sample each of the factors under consideration.

6.1. Future Work

Some of the questions raised by the analysis of the results presented here call for future research to be conducted. One of the most interesting results of this study has to do with the use of the flush mounted pressure transducers in the mold. This instrument revealed a significant pressure dependence that merits further work. These pressure transducers could be used to quantify acceptable and unacceptable leak rates, critical leak rate values, and to investigate the pressure dependence of porosity content. In order to conduct this research, a series of plates would need to be manufactured using a valve to control the leak rate. This controlled leak process could then be varied through a range a values of up to 8 – 10 laminates, and a correlation between porosity content and leak rate established by processing the laminates using SEM image analysis as was conducted for this research. Through qualitative and quantitative analysis of these plates critical leak rate could be established as protocol for subsequent student researchers. This leak rate to porosity correlation could also be extended to the subscale test fixture samples that the MSU composites group is beginning to develop.

Another important area to investigate would be to continue to improve on the models created for this research by manufacturing more laminates with different parameters than those used to generate the multivariate polynomial regression model. Using the same conditions, work could continue towards a full factorial set of laminates for the parameters under consideration in this report. This would require another 120 laminates to be manufactured using the same parameters developed in chapter 3. Also two or three repeats of the same 8 laminates manufactured for this study would give insight into the achievability of consistent results under controlled circumstances and would strengthen the current model.

Research conducted for this study has shown that the final vacuum pressure was always constant, and, therefore, the analysis results show that fiber volume fraction has very little dependence on final vacuum pressure. However, further investigation into alternative experimental configurations might show that the fiber volume fraction has a higher dependence on pressure than indicated by this study. One such configuration could employ a double-bagging method. Laminates could be manufactured with a second bag over the first that would pull a constant vacuum pressure over the first bag during the infusion process. This would provide a consistent pressure to all parts of the pre-form as it is being infused and could result in high fiber volume fractions and thus lighter parts.

The introduction of wave flaws into laminates proposed some challenges and also merits possible further investigation. It seems as though waves are hard to reproduce due to the limitations in the size of the mold. If a larger 3-D mold could be used perhaps wave flaws would be more likely to occur from mishandling or placing fabric in the mold. Also researchers could benefit from spending more time on the floor of actual blade manufacturing facilities to study the processes used.

Finally the modeling efforts presented here have the potential to predict the outcome of laminates based on various process parameters. It would be beneficial to incorporate these models into the manufacturing process not only to educate future researchers in order to produce quality laminates but also to validate the tool and potentially increase its accuracy.

Wind turbine blade manufacturers experience high capital losses due to the premature failure of blades in the field as a result of manufacturing flaws. Much of the process of manufacturing these laminates requires the knowledge and expertise of professional laminate technicians. Often their knowledge is lost with the transition to new, less experienced employees. Heuristic knowledge acquisition and quantifiable process monitoring techniques can be used to educate technicians and diagnose laminate flaws.

REFERENCES

[1] D. S. Cairns, D. R. Humbert, and J. F. Mandell, “Modeling of resin transfer molding of composite materials with oriented unidirectional plies,” *Composites Part A: Applied Science and Manufacturing,* vol. 30, no. 3, pp. 375-383, 3//, 1999.

[2] B. Gourichon, C. Binetruy, and P. Krawczak, “A new numerical procedure to predict dynamic void content in liquid composite molding,” *Composites Part A: Applied Science and Manufacturing,* vol. 37, no. 11, pp. 1961-1969, 11//, 2006.

[3] K. Han, S. Jiang, C. Zhang, and B. Wang, “Flow modeling and simulation of SCRIMP for composites manufacturing,” *Composites Part A: Applied Science and Manufacturing,* vol. 31, no. 1, pp. 79-86, 1//, 2000.

[4] J. Li, C. Zhang, Z. Liang, and B. Wang, “Stochastic simulation based approach for statistical analysis and characterization of composites manufacturing processes,” *Journal of Manufacturing Systems,* vol. 25, no. 2, pp. 108-121, //, 2006.

[5] M. Y. Lin, M. J. Murphy, and H. T. Hahn, “Resin transfer molding process optimization,” *Composites Part A: Applied Science and Manufacturing,* vol. 31, no. 4, pp. 361-371, 4//, 2000.

[6] E. Ruiz, V. Achim, S. Soukane, F. Trochu, and J. Bréard, “Optimization of injection flow rate to minimize micro/macro-voids formation in resin transfer molded composites,” *Composites Science and Technology,* vol. 66, no. 3–4, pp. 475-486, 3//, 2006.

[7] S. R. White, and H. T. Hahn, “Process Modeling of Composite Materials: Residual Stress Development during Cure. Part I. Model Formulation,” *Journal of Composite Materials,* vol. 26, no. 16, pp. 2402-2422, 1992.

[8] L. Woo Il, and G. S. Springer, “A Model of the Manufacturing Process of Thermoplastic Matrix Composites,” *Journal of Composite Materials,* vol. 21, no. 11, pp. 1017-1055, November 1, 1987, 1987.

[9] J.-S. Chou, and W.-T. Tu, “Failure analysis and risk management of a collapsed large wind turbine tower,” *Engineering Failure Analysis,* vol. 18, no. 1, pp. 295-313, 1//, 2011.

[10] J.-S. Chou, C.-K. Chiu, I. K. Huang, and K.-N. Chi, “Failure analysis of wind turbine blade under critical wind loads,” *Engineering Failure Analysis,* vol. 27, no. 0, pp. 99-118, 1//, 2013.

[11] J. Nelson, D. Cairns, and T. Riddle, "Manufacturing Defects Common to Composite Wind Turbine Blades: Effects of Defects," *52nd AIAA/ASME/ASCE/AHS/ASC Structures, Structural Dynamics and Materials Conference*, Structures, Structural Dynamics, and Materials and Co-located Conferences: American Institute of Aeronautics and Astronautics, 2011.

[12] W. Kyeongsik, J. Nelson, D. Cairns, and T. Riddle, "Effects of Defects: Part B?Progressive Damage Modeling of Fiberglass/Epoxy Composite Structures with Manufacturing Induced Flaws Utilizing Cohesive Zone Elements," *54th AIAA/ASME/ASCE/AHS/ASC Structures, Structural Dynamics, and Materials Conference*, Structures, Structural Dynamics, and Materials and Co-located Conferences: American Institute of Aeronautics and Astronautics, 2013.

[13] T. Riddle, D. Cairns, and J. Nelson, "Characterization of Manufacturing Defects Common to Composite Wind Turbine Blades: Flaw Characterization," *52nd AIAA/ASME/ASCE/AHS/ASC Structures, Structural Dynamics and Materials Conference*, Structures, Structural Dynamics, and Materials and Co-located Conferences: American Institute of Aeronautics and Astronautics, 2011.

[14] T. Riddle, D. Cairns, S., and J. Nelson, "Effects of Defects Part A: Stochastic Finite Element Modeling of Wind Turbine Blades with Manufacturing Defects for Reliability Estimation," *54th AIAA/ASME/ASCE/AHS/ASC Structures, Structural Dynamics, and Materials Conference*, Structures, Structural Dynamics, and Materials and Co-located Conferences: American Institute of Aeronautics and Astronautics, 2013.

[15] E. C. Meehan, "Development of embedded sensors for structural health monitiroing of wind turbine blades," 2012, pp. xii, 93 leaves.
[16] I. Abundez Barrera, E. Rendón Lara, C. Gutiérrez Estrada, and S. Díaz Zagal, "Diagnosis of Medical Images Using an Expert System," *Advances in Artificial Intelligence – IBERAMIA 2010*, Lecture Notes in Computer Science A. Kuri-Morales and G. Simari, eds., pp. 144-152: Springer Berlin Heidelberg, 2010.
[17] H. A. L. Lemmon, "Comax: An Expert System for Cotton Crop Management," *Science,* vol. 233, no. 4759, pp. 29-33, 1986.
[18] S. Mitra, S. K. Saha, and N. K. Ghosh, "Application of expert system for heating control of Annealing Furnaces in a cold rolling mill — A case study at Bokaro Steel Plant." pp. 245-249.
[19] W. Zhang, and B. T. Chait, "ProFound: An Expert System for Protein Identification Using Mass Spectrometric Peptide Mapping Information," *Analytical Chemistry,* vol. 72, no. 11, pp. 2482-2489, 2000/06/01, 2000.
[20] L. Bird, M. Bolinger, T. Gagliano, R. Wiser, M. Brown, and B. Parsons, "Policies and market factors driving wind power development in the United States," *Energy Policy,* vol. 33, no. 11, pp. 1397-1407, 7//, 2005.
[21] K. J. Jackson, M. D. Zuteck, C. P. van Dam, K. J. Standish, and D. Berry, "Innovative design approaches for large wind turbine blades," *Wind Energy,* vol. 8, no. 2, pp. 141-171, 2005.
[22] P. S. Veers, T. D. Ashwill, H. J. Sutherland, D. L. Laird, D. W. Lobitz, D. A. Griffin, J. F. Mandell, W. D. Musial, K. Jackson, M. Zuteck, A. Miravete, S. W. Tsai, and J. L. Richmond, "Trends in the Design, Manufacture and Evaluation of Wind Turbine Blades," *Wind Energy,* vol. 6, no. 3, pp. 245-259, 2003.
[23] E. J. Barbero, *Introduction to Composite Materials Design*: Taylor & Francis Group, 2011.
[24] P. Brøndsted, H. Lilholt, and A. Lystrup, "COMPOSITE MATERIALS FOR WIND POWER TURBINE BLADES," *Annual Review of Materials Research,* vol. 35, no. 1, pp. 505-538, 2005/08/04, 2005.
[25] "An investigation into a damaged wind turbine revealed the cause was a defect in the manufacturing of a blade. (TB file photo)."
[26] Momentive. "Technical Data Sheet," http://www.momentive.com/Products/TechnicalDataSheet.aspx?id=8246.
[27] A. Abbassi, and M. R. Shahnazari, "Numerical modeling of mold filling and curing in non-isothermal RTM process," *Applied Thermal Engineering,* vol. 24, no. 16, pp. 2453-2465, 11//, 2004.
[28] N. Kuentzer, P. Simacek, S. G. Advani, and S. Walsh, "Correlation of void distribution to VARTM manufacturing techniques," *Composites Part A: Applied Science and Manufacturing,* vol. 38, no. 3, pp. 802-813, 3//, 2007.
[29] D. B. Mastbergen, "Simulation and testing of resin infusion manufacturing processes for large composite structures," 2004, pp. xi, 154 leaves.
[30] O. Restrepo, K.-T. Hsiao, A. Rodriguez, and B. Minaie, "Development of adaptive injection flow rate and pressure control algorithms for resin transfer molding," *Composites Part A: Applied Science and Manufacturing,* vol. 38, no. 6, pp. 1547-1568, 6//, 2007.
[31] J. Samir, J. Echaabi, and M. Hattabi, "Numerical algorithm and adaptive meshing for simulation the effect of variation thickness in resin transfer molding process," *Composites Part B: Engineering,* vol. 42, no. 5, pp. 1015-1028, 7//, 2011.
[32] D. H. Lee, W. I. Lee, and M. K. Kang, "Analysis and minimization of void formation during resin transfer molding process," *Composites Science and Technology,* vol. 66, no. 16, pp. 3281-3289, 12/18/, 2006.
[33] R. K. Roy, *A primer on the Taguchi method*, New York: Van Nostrand Reinhold, 1990.

[34] B. Gourichon, C. Binetruy, and P. Krawczak, "Experimental investigation of high fiber tow count fabric unsaturation during RTM," *Composites Science and Technology,* vol. 66, no. 7–8, pp. 976-982, 6//, 2006.
[35] W. Gu, H. F. Wu, S. L. Kampe, and G. Q. Lu, "Volume fraction effects on interfacial adhesion strength of glass-fiber-reinforced polymer composites," *Materials Science and Engineering: A,* vol. 277, no. 1–2, pp. 237-243, 1/31/, 2000.
[36] S. V. Joshi, L. T. Drzal, A. K. Mohanty, and S. Arora, "Are natural fiber composites environmentally superior to glass fiber reinforced composites?," *Composites Part A: Applied Science and Manufacturing,* vol. 35, no. 3, pp. 371-376, 3//, 2004.

APPENDIX A: TAGUCHI DESIGN MATRIX

Factors:
NFL – number of layers of flow media
FAA – fabric architecture
NFA – number of layers of fabric
IFR – injection flow rate
ITS – injection temperature (start)
VPS – vacuum pressure (start)
DGR – degassed resin

Number of levels for each factor: n:=7 **Number of factors:** 1:=2

Build a Taguchi design matrix:
X := taguchi(n,1)

Define the correlation between the factors and there level variation in matrix form:

Vals :=

"NFL"	1	3
"FAA"	"Triax"	"Uni"
"NFA"	2	6
"IFR"	"low"	"high"
"ITS"	"low"	"high"
"VPS"	"low"	"high"
"DGR"	"no"	"yes"

Substitute level values into Taguchi design matrix.

D := doelabel(X,Vals)

Design matrix with the level values filled in:

D =

"Run"	"Block"	"NFL"	"FAA"	"NFA"	"IFR"	"ITS"	"VPS"	"DGR"
1	1	1	"Triax"	2	"low"	"low"	"low"	"no"
2	1	1	"Triax"	2	"high"	"high"	"high"	"yes"
3	1	1	"Uni"	6	"low"	"low"	"high"	"yes"
4	1	1	"Uni"	6	"high"	"high"	"low"	"no"
5	1	3	"Triax"	6	"low"	"high"	"low"	"yes"
6	1	3	"Triax"	6	"high"	"low"	"high"	"no"
7	1	3	"Uni"	2	"low"	"high"	"high"	"no"
8	1	3	"Uni"	2	"high"	"low"	"low"	"yes"

APPENDIX B: Transducer Calibration

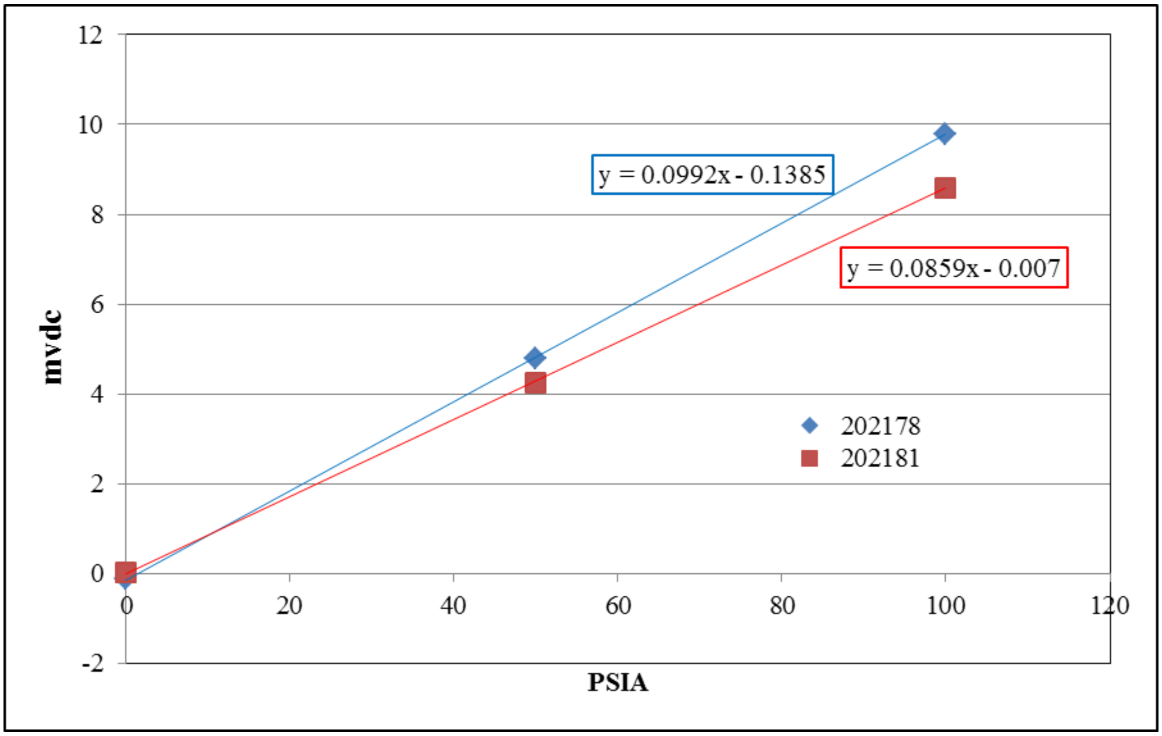

This chart shows the transducer calibration curve for each of the transducers used in this experiment.

APPENDIX C: PARAMETER DATA MONITORED

C.1: Raw Data from Mass Balance

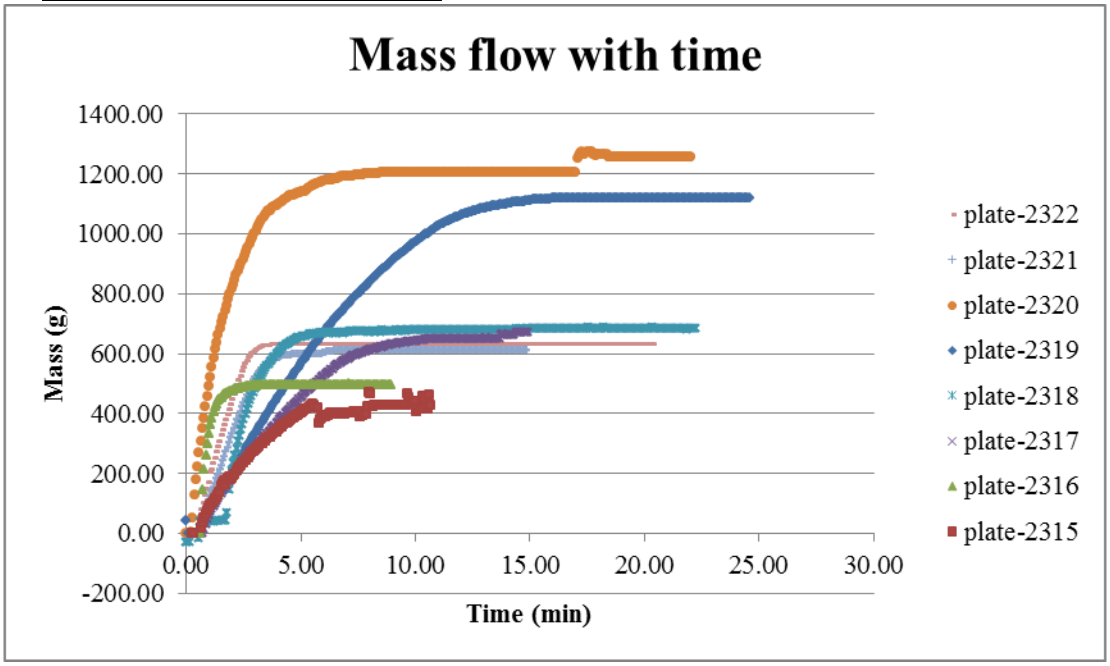

This chart shows the raw data from the scale for the various different plates that were manufactured

C.2: Calculated Flow Rate Through the Laminate

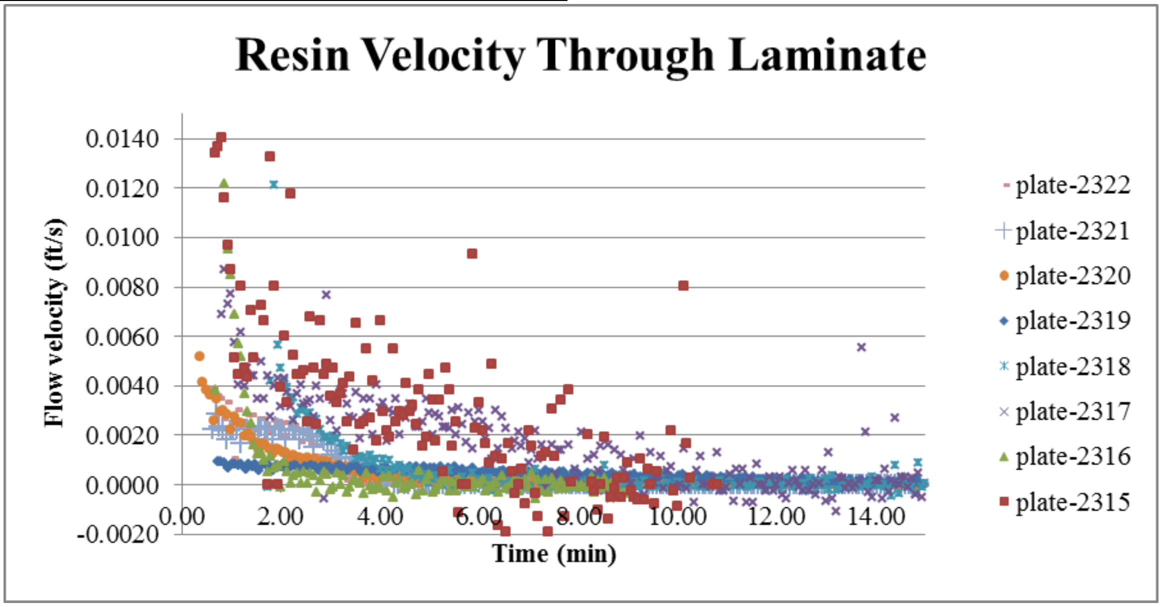

This chart shows the calculated flow rate through the laminate taking into account the varying thicknesses of the different laminates.

C.3: Pressure Transducer Data

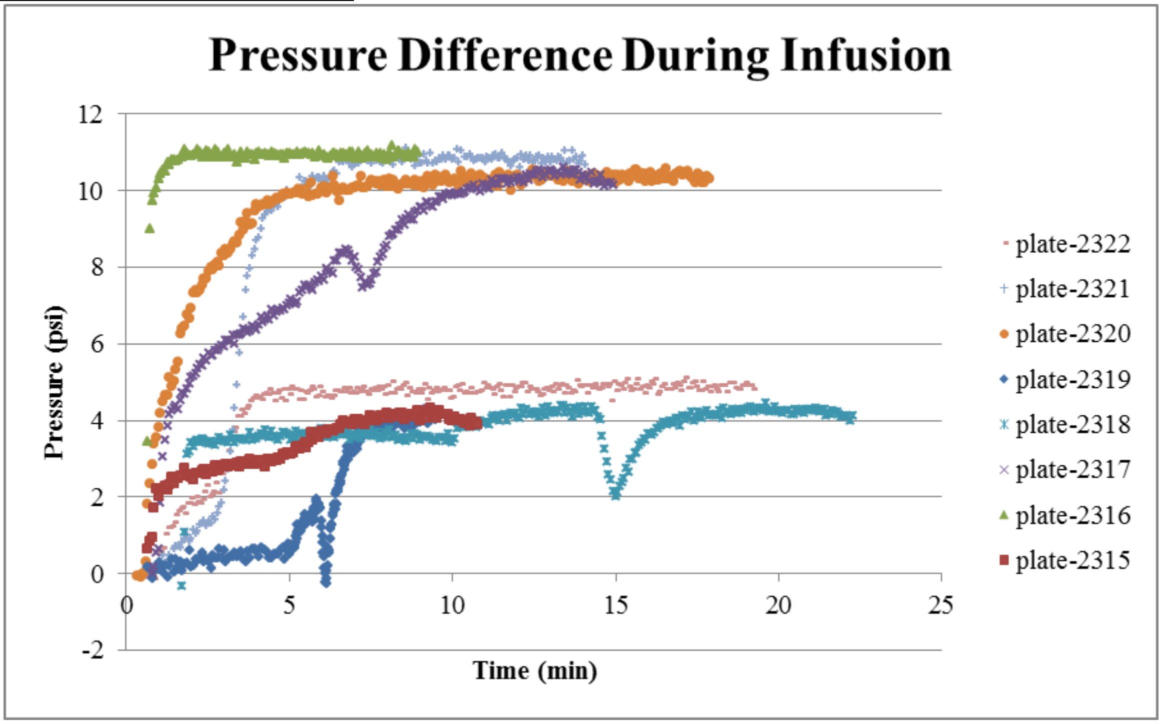

This chart shows the pressure difference between the inlet and outlet ports of the mold during the infusion process.

The following charts depict the actual raw data from the two pressure transducers with values converted to pounds per square in and plotted against time.

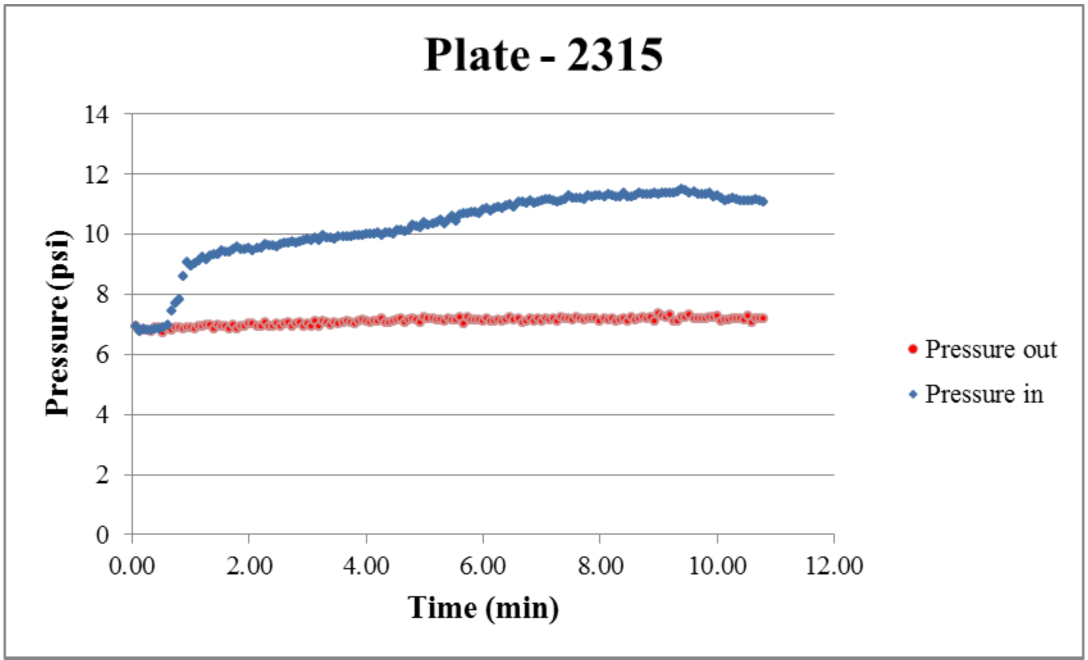

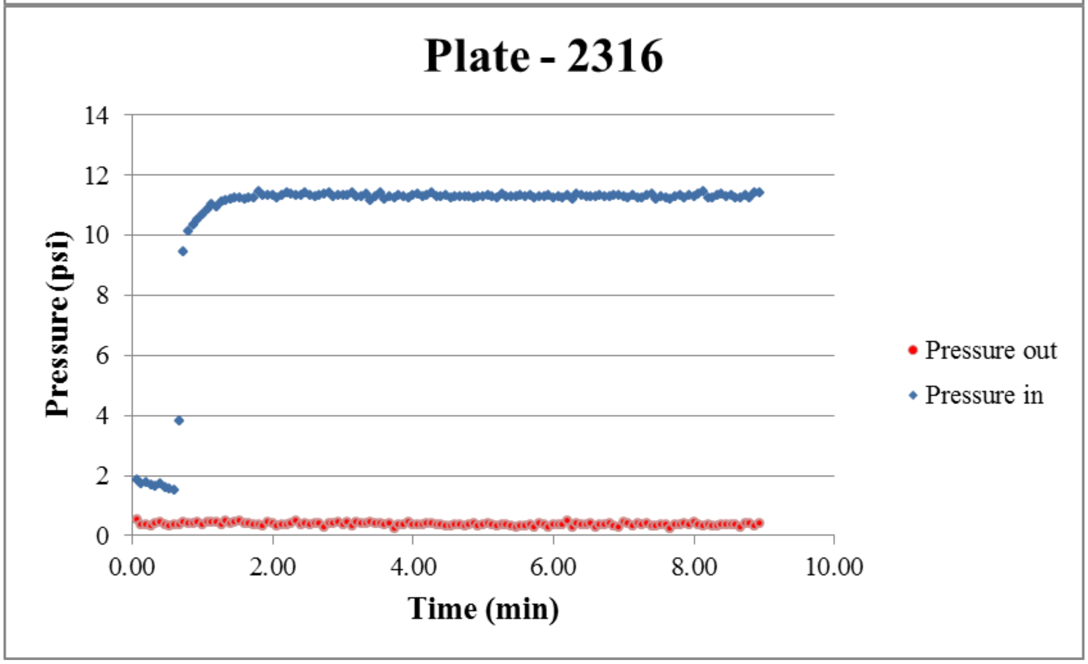

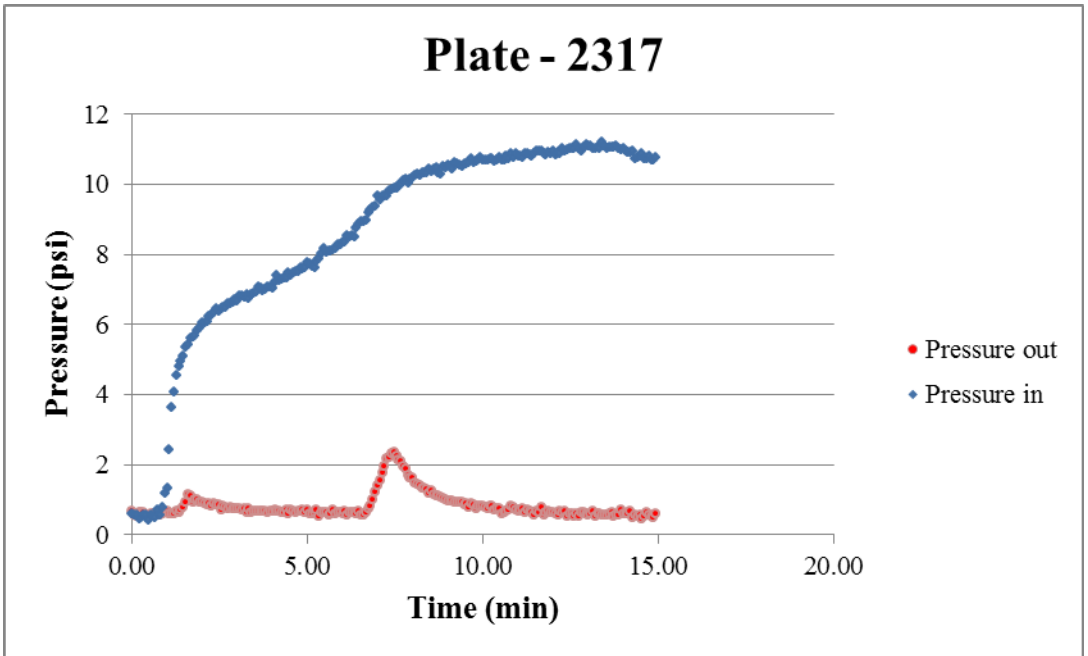
Plate - 2317
Pressure (psi)
Time (min)
0
2
4
6
8
10
12
0.00
5.00
10.00
15.00
20.00
Pressure out
Pressure in

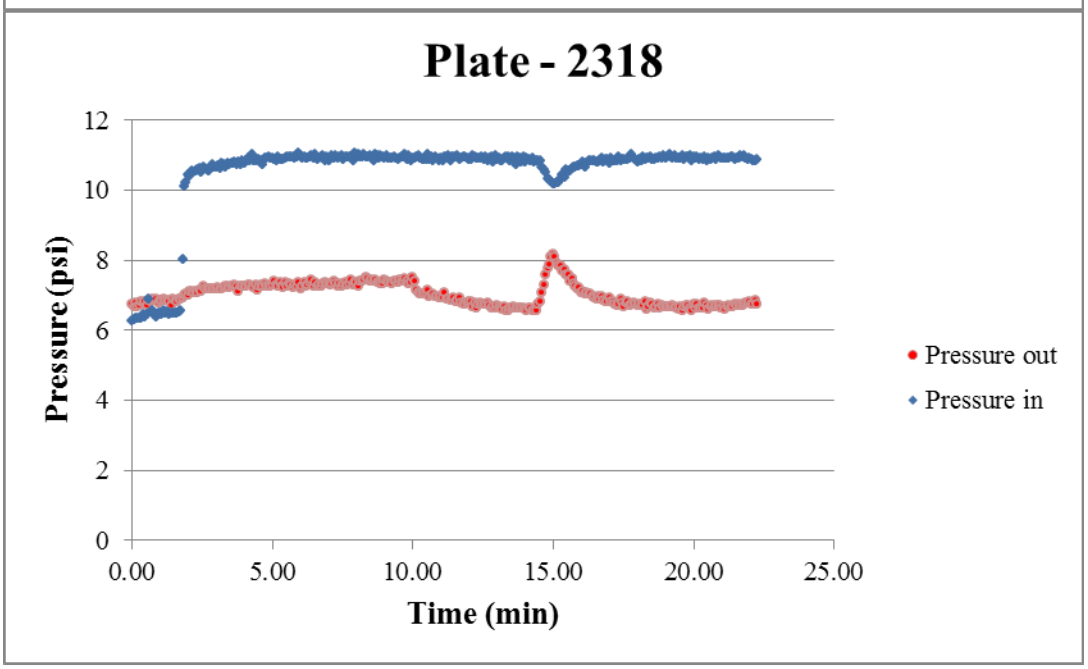
Plate - 2318
Pressure (psi)
Time (min)
0
2
4
6
8
10
12
0.00
5.00
10.00
15.00
20.00
25.00
Pressure out
Pressure in

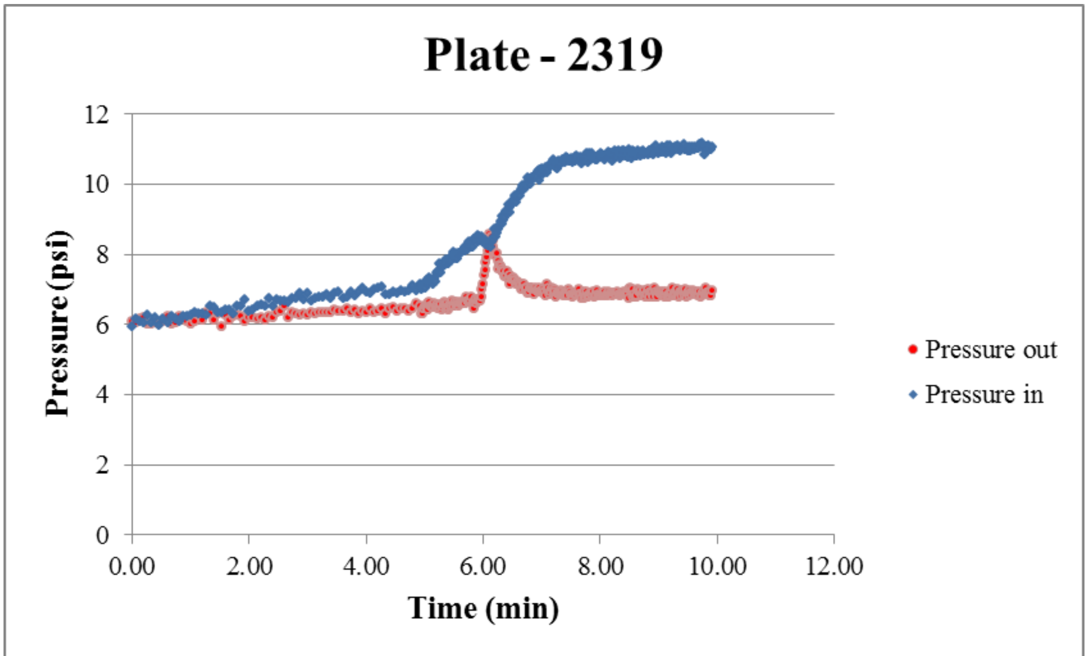

Plate - 2319
Pressure (psi)
Time (min)
0
2
4
6
8
10
12
0.00
2.00
4.00
6.00
8.00
10.00
12.00
Pressure out
Pressure in

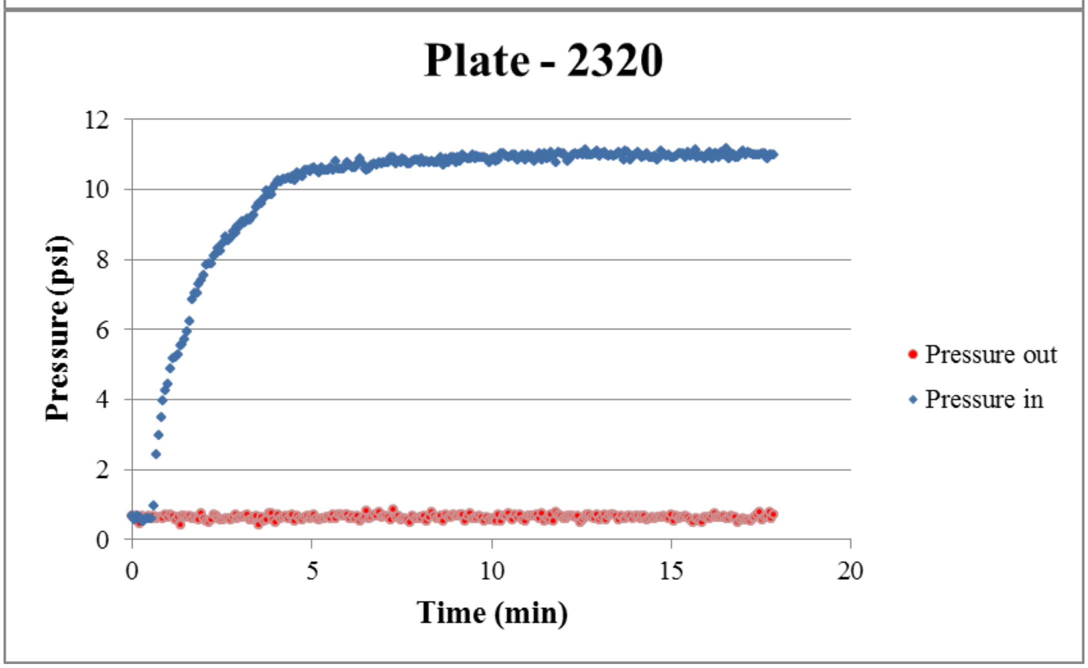

Plate - 2320
Pressure (psi)
Time (min)
0
2
4
6
8
10
12
0
5
10
15
20
Pressure out
Pressure in

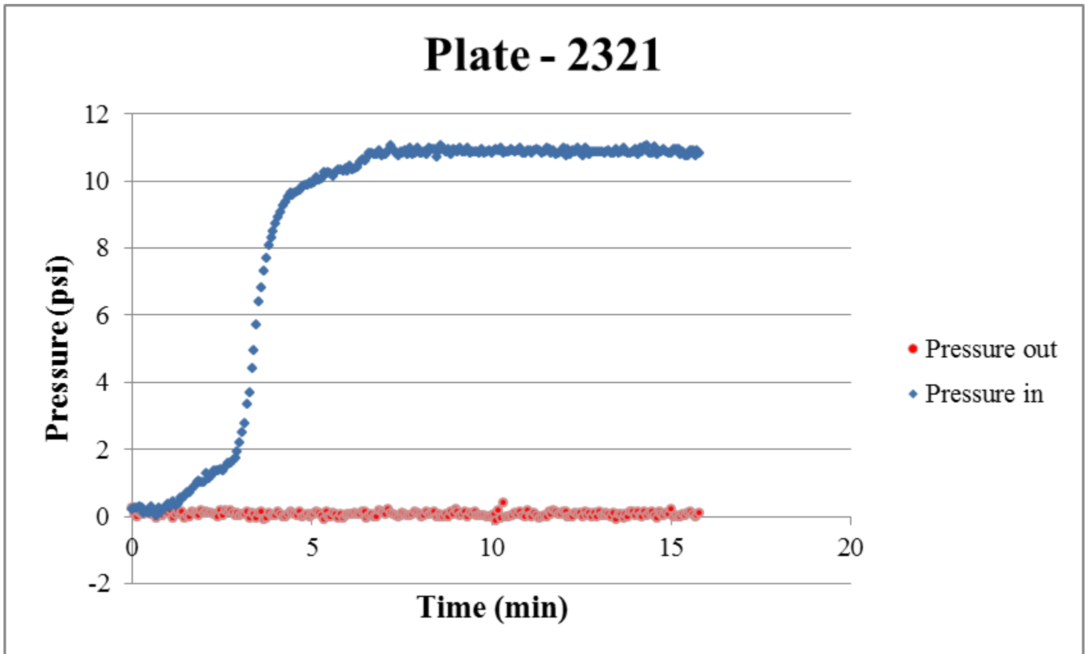
Plate - 2321
Pressure (psi)
12
10
8
6
4
2
0
-2
0
5
10
15
20
Time (min)
Pressure out
Pressure in

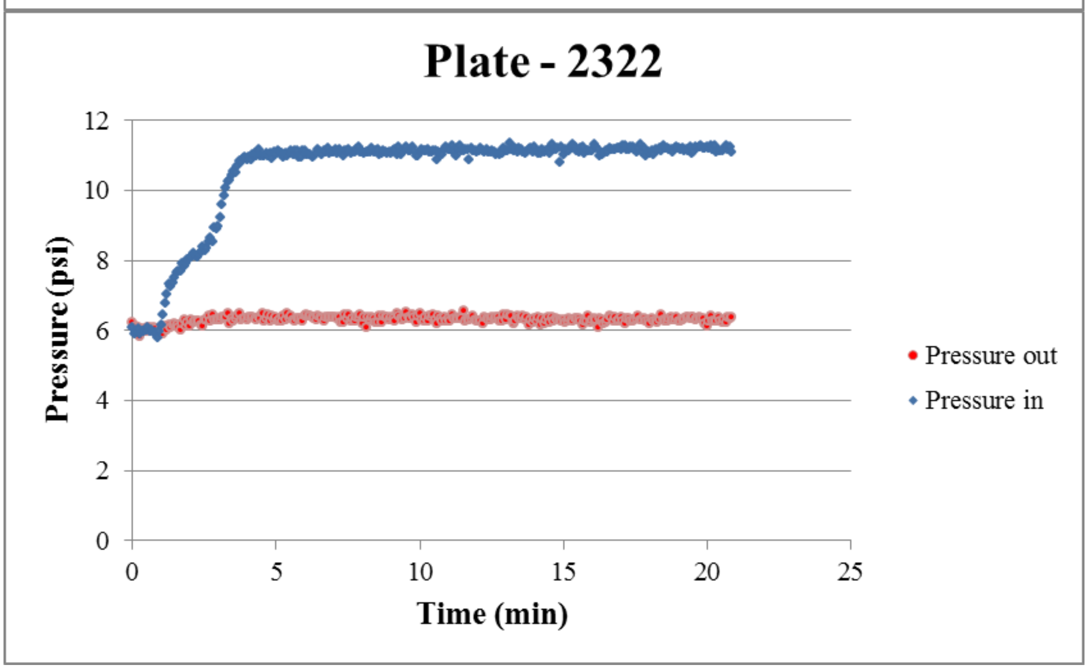
Plate - 2322
Pressure (psi)
12
10
8
6
4
2
0
0
5
10
15
20
25
Time (min)
Pressure out
Pressure in

C.4: Infrared Sensor Temperature Profile

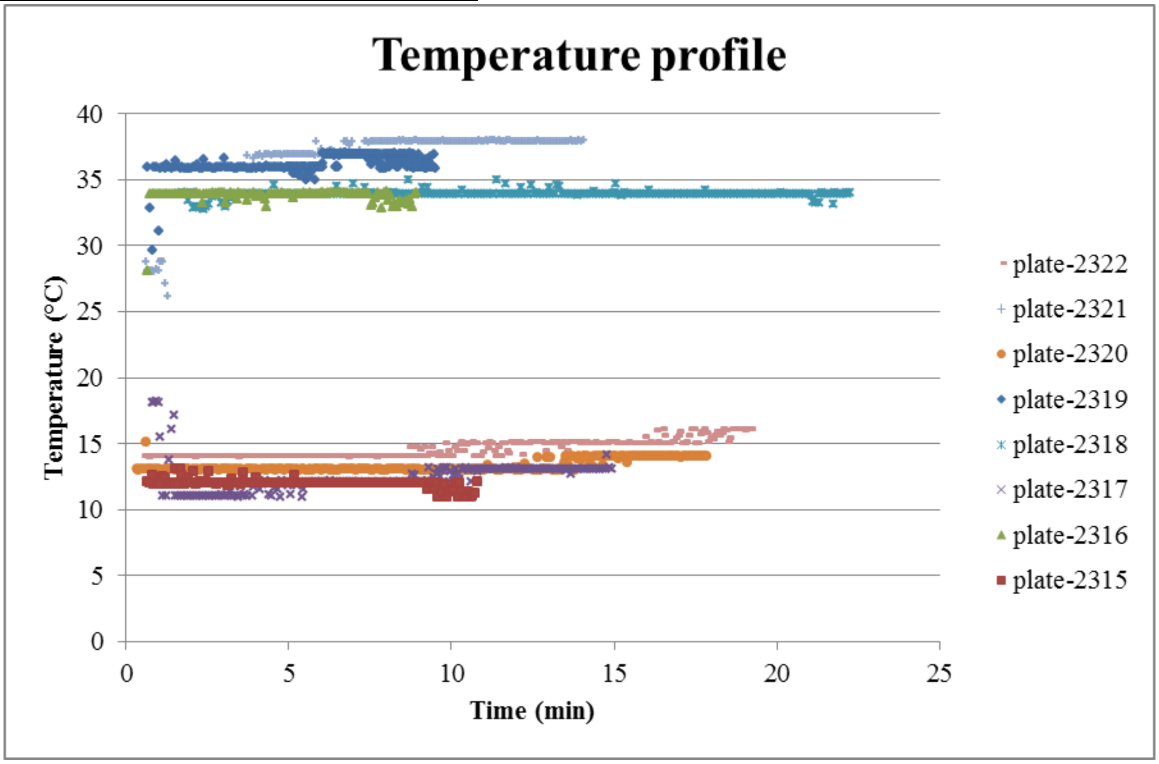

This chart depicts the temperature of the resin in the bucket during the process of injection.

APPENDIX D: IMAGE J MACROS

D.1: Macro for Creating Overlay Image

```
makeRectangle(0, 0, 2000, 1420);
run("Crop");
run("8-bit");
saveAs("Tiff", "C:\\Users\\daniel.guest\\SkyDrive\\Documents\\Grad school stuff\\my research\\supporting pictures\\SEM pics\\sample pics\\2320\\cropped\\2320-7-a-1.tif");
```

D.2: Macro for Creating Binary Image

```
makeRectangle(0, 0, 2000, 1420);
run("Crop");
run("8-bit");
run("Subtract...", "value=180");
run("Multiply...", "value=255");
run("Remove Outliers...", "radius=4 threshold=0 which=Bright");
run("Fill Holes");
run("Add Image...", "image=2320-7-a-1.tif x=0 y=0 opacity=60");
```

APPENDIX E: VALIDATION OF FIBER VOLUME FRACTION MODEL

<u>Validation of fiber volume results using model:</u>

Prediction of parameters from run 1:	$V_f\left(In^{\langle 1 \rangle}\right) = 48$	Actual value = 48%
Prediction of parameters from run 2:	$V_f\left(In^{\langle 2 \rangle}\right) = 45$	Actual value = 45%
Prediction of parameters from run 3:	$V_f\left(In^{\langle 3 \rangle}\right) = 56$	Actual value = 56%
Prediction of parameters from run 4:	$V_f\left(In^{\langle 4 \rangle}\right) = 55$	Actual value = 55%
Prediction of parameters from run 5:	$V_f\left(In^{\langle 5 \rangle}\right) = 52$	Actual value = 52%
Prediction of parameters from run 6:	$V_f\left(In^{\langle 6 \rangle}\right) = 52$	Actual value = 52%
Prediction of parameters from run 7:	$V_f\left(In^{\langle 7 \rangle}\right) = 55$	Actual value = 55%
Prediction of parameters from run 8:	$V_f\left(In^{\langle 8 \rangle}\right) = 54$	Actual value = 54%

APPENDIX F: CLIPS CODE FOR IMPLEMENTATION OF EXPERT SYSTEM

```
;;;======================================================
;;;   Flaw Identification Expert System
;;;
;;;     A simple expert system which attempts to identify
;;;     the source of prosity/wave flaws in laminates based on characteristics
;;;    of the laminate manufacturing process.
;;;
;;;     To execute, merely load, reset, and run.
;;;     Answer questions yes or no.
;;;======================================================

;;;***************************
;;;* DEFTEMPLATE DEFINITIONS *
;;;***************************

(deftemplate rule
   (multislot if)
   (multislot then))

;;;**************************
;;;* INFERENCE ENGINE RULES *
;;;**************************

(defrule propagate-goal ""
   (goal is ?goal)
   (rule (if ?variable $?)
         (then ?goal ? ?value))
   =>
   (assert (goal is ?variable)))

(defrule goal-satified ""
   (declare (salience 30))
   ?f <- (goal is ?goal)
   (variable ?goal ?value)
   (answer ? ?text ?goal)
   =>
   (retract ?f)
   (format t "%s%s%n" ?text ?value))

(defrule remove-rule-no-match ""
   (declare (salience 20))
   (variable ?variable ?value)
   ?f <- (rule (if ?variable ? ~?value $?))
   =>
   (retract ?f))

(defrule modify-rule-match ""
   (declare (salience 20))
   (variable ?variable ?value)
   ?f <- (rule (if ?variable ? ?value and $?rest))
   =>
   (modify ?f (if ?rest)))

(defrule rule-satisfied ""
   (declare (salience 20))
   (variable ?variable ?value)
   ?f <- (rule (if ?variable ? ?value)
               (then ?goal ? ?goal-value))
   =>
```

```
   (retract ?f)
   (assert (variable ?goal ?goal-value)))

(defrule ask-question-no-legalvalues ""
   (declare (salience 10))
   (not (legalanswers $?))
   ?f1 <- (goal is ?variable)
   ?f2 <- (question ?variable ? ?text)
   =>
   (retract ?f1 ?f2)
   (format t "%s " ?text)
   (assert (variable ?variable (read))))

(defrule ask-question-legalvalues ""
   (declare (salience 10))
   (legalanswers ? $?answers)
   ?f1 <- (goal is ?variable)
   ?f2 <- (question ?variable ? ?text)
   =>
   (retract ?f1)
   (format t "%s " ?text)
   (printout t ?answers " ")
   (bind ?reply (read))
   (if (member (lowcase ?reply) ?answers)
     then (assert (variable ?variable ?reply))
          (retract ?f2)
     else (assert (goal is ?variable))))

;;;***************************
;;;* DEFFACTS KNOWLEDGE BASE *
;;;***************************

(deffacts knowledge-base
   (goal is flaw.global)
   (legalanswers are yes no)
   (rule (if q-1 is yes)
         (then flaw.type is porosity))
   (rule (if q-1 is no)
         (then flaw.type is waves))
   (question q-1 is "Is your laminate flawed with porosity/white spots?")
   (rule (if flaw.type is porosity and
         q-2 is yes)
         (then porosity.type is leak))
   (rule (if flaw.type is porosity and
         q-2 is no)
         (then porosity.type is methods))
   (question q-2 is "Are there air pockets in flow media?")
   (rule (if flaw.type is porosity and
         q-3 is yes)
         (then flaw.global is "The leak is most likely caused from insufficient
clamping pressure or ports not well sealed."))
   (rule (if flaw.type is porosity and
         q-3 is no)
         (then leak.ports is other))
   (question q-3 is "Are there air pockets in the ports?")
   (rule (if flaw.type is porosity and
         q-4 is yes)
         (then leak.seal is seal))
   (rule (if flaw.type is porosity and
         q-4 is no)
         (then leak.seal is sealed))
   (question q-4 is "During resin infusion did you notice air bubbles traveling from
the tacky tape inward toward the laminate or vacuum port?")
```

```
   (rule (if leak.seal is seal and
         q-5 is yes)
          (then flaw.global is "The leak is most likely caused from fibers under the tacky tape disrupting the seal."))
   (rule (if leak.seal is seal and
         q-5 is no)
          (then flaw.global is "The leak is most likely caused from improper seal between the mold and bag."))
   (question q-5 is "Are there fibers under the tacky tape?")
   (rule (if leak.seal is seal and
         q-6 is yes)
          (then flaw.global is "The leak is most likely caused from not compressing the tacky tape overlap at the corners."))
   (rule (if leak.seal is seal and
         q-6 is no)
          (then flaw.global is "The leak is most likely caused from improper seal between the mold and bag."))
   (question q-6 is "Does the leak appear to originate at a corner?")
   (rule (if leak.seal is seal and
         q-7 is yes)
          (then flaw.global is "The leak is most likely caused from not completely sealing the pleat."))
   (rule (if leak.seal is seal and
         q-7 is no)
          (then flaw.global is "The leak is most likely caused from improper seal between the mold and bag."))
   (question q-7 is "Does the leak appear to originate at a pleat?")
   (rule (if leak.seal is sealed and
          q-8 is yes)
         (then flaw.global is "The leak may have originated from a hole in the bag."))
   (rule (if leak.seal is sealed and
          q-8 is no)
         (then flaw.global is "The leak is from undetermined seal problem."))
   (question q-8 is "Is the porosity localized/not dispersed throughout the laminate?")
   (rule (if porosity.type is methods and
          q-9 is yes)
         (then flaw.global is "Porosity could be caused by the insertion of sensors or forgien objects."))
   (rule (if porosity.type is methods and
          q-9 is no)
         (then flaw.global is "Processing parameters are likely the cause of porosity, the two most significant of which are vauum pressure and flow rate."))
   (question q-9 is "Is the porosity localized to a spot or a line?")
   (rule (if flaw.type is waves and
          q-9 is yes)
         (then flaw.global is "The out-of-plane wave is most likely caused by a foriegn imedded object"))
   (rule (if flaw.type is waves and
          q-9 is no)
         (then flaw.global is "The in-plane wave is most likely caused by mishandling the fabic."))
   (question q-9 is "Is there a bump on the surface of the laminate?")
   (answer is " "flaw.global))
```

Distribution:
MS 0899 Technical Library, 9536 (electronic copy)

Sandia National Laboratories